

Alma Mater Studiorum Università di Bologna
Archivio istituzionale della ricerca

Discovery of novel benzofuran-based compounds with neuroprotective and immunomodulatory properties for Alzheimer's disease treatment

This is the final peer-reviewed author's accepted manuscript (postprint) of the following publication:

Published Version:

Montanari S., Mahmoud A.M., Pruccoli L., Rabbito A., Naldi M., Petralla S., et al. (2019). Discovery of novel benzofuran-based compounds with neuroprotective and immunomodulatory properties for Alzheimer's disease treatment. EUROPEAN JOURNAL OF MEDICINAL CHEMISTRY, 178, 243-258 [10.1016/j.ejmech.2019.05.080].

Availability:

This version is available at: <https://hdl.handle.net/11585/700770> since: 2020-02-13

Published:

DOI: <http://doi.org/10.1016/j.ejmech.2019.05.080>

Terms of use:

Some rights reserved. The terms and conditions for the reuse of this version of the manuscript are specified in the publishing policy. For all terms of use and more information see the publisher's website.

This item was downloaded from IRIS Università di Bologna (<https://cris.unibo.it/>).
When citing, please refer to the published version.

(Article begins on next page)

This is the final peer-reviewed accepted manuscript of:

Montanari S, Mahmoud AM, Pruccoli L, et al. Discovery of novel benzofuran-based compounds with neuroprotective and immunomodulatory properties for Alzheimer's disease treatment. *Eur J Med Chem.* 2019;178:243-258. doi:10.1016/j.ejmech.2019.05.080

The final published version is available online at:
<http://dx.doi.org/10.1016/j.ejmech.2019.05.080>

Rights / License:

The terms and conditions for the reuse of this version of the manuscript are specified in the publishing policy. For all terms of use and more information see the publisher's website.

This item was downloaded from IRIS Università di Bologna (<https://cris.unibo.it/>)

When citing, please refer to the published version.

DISCOVERY OF NOVEL BENZOFURAN-BASED COMPOUNDS WITH NEUROPROTECTIVE AND IMMUNOMODULATORY PROPERTIES FOR ALZHEIMER'S DISEASE TREATMENT

Serena Montanari,¹ Ali Mokhtar Mahmoud,² Letizia Pruccoli,³ Alessandro Rabbito,² Marina Naldi,¹ Sabrina Petralla,¹ Ignacio Moraleda,⁴ Manuela Bartolini,¹ Barbara Monti,¹ Isabel Iriepa,^{4,5} Federica Belluti,¹ Silvia Gobbi,¹ Vincenzo Di Marzo,² Alessandra Bisi,¹ Andrea Tarozi,³ Alessia Ligresti,² Angela Rampa^{1*}

¹*Department of Pharmacy and Biotechnology, Alma Mater Studiorum-University of Bologna, Via Belmeloro 6, 40126 Bologna, Italy;* ²*Endocannabinoid Research Group, Institute of Biomolecular Chemistry, National Research Council, Via Campi Flegrei 34, 80078 Pozzuoli, NA, Italy;* ³*Department for Life Quality Studies, Alma Mater Studiorum-University of Bologna, Corso d'Augusto 237, 47921 Rimini, Italy;* ⁴*Departamento de Química Orgánica y Química Inorgánica, Universidad de Alcalá, 28805-Alcalá de Henares, Madrid, Spain;* ⁵*Instituto de Investigación Química Andrés M. del Río (IQAR), Universidad de Alcalá, 28805-Alcalá de Henares, Madrid, Spain*

Corresponding Author

*Phone: +39-051-2099710. Fax: +39-051-2099734. E-mail: angela.rampa@unibo.it.

This item was downloaded from IRIS Università di Bologna (<https://cris.unibo.it/>)

When citing, please refer to the published version.

Abbreviations: Alzheimer's disease (AD); acetylcholinesterase (AChE); butyrylcholinesterase (BuChE); multi-target-directed ligands (MTDLs); endocannabinoid system (ECS); inducible nitric oxide synthase (iNOS); triggering receptor expressed on myeloid cells 2 (TREM2); lipopolysaccharide (LPS); Glyceraldehyde 6-phosphate dehydrogenase (GAPDH)

This item was downloaded from IRIS Università di Bologna (<https://cris.unibo.it/>)

When citing, please refer to the published version.

Abstract

To address the multifactorial nature of Alzheimer's Disease (AD), a multi-target-directed ligand approach was herein developed. As a follow-up of our previous studies, a small library of newly designed 2-arylbenzofuran derivatives was evaluated for its biological activities towards cholinesterases and cannabinoid receptors. The two most promising compounds, **8** and **10**, were then assessed for their neuroprotective activity and for their ability to modulate the microglial phenotype. Compound **8** emerged as able to fight AD from several directions: it restored the cholinergic system by inhibiting butyrylcholinesterase, showed neuroprotective activity against A β ₁₋₄₂ oligomers, was a potent and selective CB₂ ligand and had immunomodulatory effects, switching microglia from the pro-inflammatory M1 to the neuroprotective M2 phenotype. Derivative **10** was a potent CB₂ inverse agonist with promising immunomodulatory properties and could be considered as a tool for investigating the role of CB₂ receptors and for developing potential immunomodulating drugs addressing the endocannabinoid system.

Keywords

MTDL; benzofuran scaffold; A β peptide; neuroprotection; CB receptors; anti-inflammatory M2 phenotype.

This item was downloaded from IRIS Università di Bologna (<https://cris.unibo.it/>)

When citing, please refer to the published version.

1. Introduction

Alzheimer's disease (AD) is the most common form of dementia, with the strongest social impact for incidence and cost of care: its debilitating nature leads to enormous financial and emotional stress on patients and caregivers. AD is the sixth leading cause of death, currently affecting more than 44 million people worldwide. Its incidence is expected to increase in the next decades due to the increase in the average age of the world population [1].

AD is a multifactorial disorder and the mechanism underlying its pathogenesis is not completely clear yet, although genetic and biochemical clues suggest that dysfunction of the basal acetylcholine (ACh) forebrain signaling [2], deposition of β -amyloid protein ($A\beta$) [3], τ protein hyperphosphorylation [4] and neuroinflammation elicited by activated microglia play a significant role in the disease. Indeed, recent studies have reported that, during the activation processes, microglia acquires different pro-inflammatory M1 and anti-inflammatory M2 phenotypes [5]. M1 phenotype, elicited by β -amyloid protein and τ hyperphosphorylation, becomes relevant at the injury site in the later stage of AD when the neurorepair role of the M2 phenotype is dampened [5]. However, in AD, microglia may also exhibit mixed activation phenotypes [6].

To date, only palliative treatments are available for AD. The limited effectiveness of current therapies highlights the need for intensifying research efforts devoted to the development of new agents for preventing or slowing down the disease progression. Management of AD through the modulation of multiple mechanisms rather than a single dysregulated pathway should have a higher chance of success [7]. Therefore, exploring novel potential therapeutic targets appears as an urgent need.

This item was downloaded from IRIS Università di Bologna (<https://cris.unibo.it/>)

When citing, please refer to the published version.

Cannabinoids also have attracted interest in AD because of the beneficial reduction the typical neurotoxic events of the disease [8]. The endocannabinoid system (ECS) is generally deemed as a part of the neuroprotective endogenous mechanisms of the central nervous system (CNS) and has been proposed as a target for the treatment of neuroinflammation. ECS is a complex system of receptors, endogenous ligands, and enzymes catalyzing ligand formation and degradation. It helps regulating fundamental processes in both central and peripheral nervous systems. ECS regulation and dysregulation might counteract disturbances of such functions [9].

To date, two subtypes of cannabinoid Gi/o-coupled receptors, CB₁ and CB₂, have been fully characterized and cloned. CB₁ is mainly present in neurons and glial cells and regulates important brain functions including cognition and memory processes. Furthermore, recent studies have revealed that CB₁ receptor density increases in early AD and decreases during later stages. Among cannabinoid receptors, the role of CB₁ is the most controversial in terms of effects on microglial activation [10]. However, recent evidence has shown that CB₁ can promote M1 polarization of monocytes/macrophages during chronic inflammatory processes [11]. Therefore, as for macrophage-like cells, the activation of CB₁ could be prodromal of the late microglia M1 phenotype in the progression of AD.

On the other hand, CB₂ receptors are localized in immune system cells and modulate their migration and the release of cytokines. Within the CNS, CB₂ receptors are mainly located in microglia, the major immune cells of the brain. Recent studies have demonstrated selective CB₂ upregulation in response to neuroinflammation, as seen during neurodegeneration. In particular, in AD patients, CB₂ are overexpressed in microglia cells surrounding A β plaques [12]. Notably, CB₂ can reduce neuroinflammation by promoting the M1 to M2 phenotype transformation in microglia [13-14].

This item was downloaded from IRIS Università di Bologna (<https://cris.unibo.it/>)

When citing, please refer to the published version.

To accomplish multifunctional compounds for the treatment of AD, a promising strategy is the molecular hybridization approach, which allows achieving multitarget-direct ligands (MTDLs) able to hit more than one biological target associated with the disease [7]. Taking this into account, we have previously demonstrated that purposely designed benzofuran derivatives can act as MTDLs towards targets involved in AD [15]. Indeed, the benzofuran scaffold is considered a privileged structure and a very important pharmacophore in drug discovery because of its presence in a great number of natural products and biologically active compounds [16]. Furthermore, the benzofuran derivatives SKF-64346 and LY320135 (Figure 1) have been shown to inhibit A β aggregation [17] and act as high affinity antagonist/inverse agonist at CB₁ receptor [18], respectively. In previous papers we reported different 2-arylbenzofuran hybrid molecules [15, 19] rationally designed to include the benzofuran scaffold and a key pharmacophore from some acetylcholinesterase/butyrylcholinesterase (AChE/BuChE) inhibitors identified in our previous studies. From this collection, compound **1** (Figure 1) emerged as a promising MTDL lead, displaying both anticholinesterase activity and anti-aggregation properties towards A β , along with neuroprotective effects towards human neuronal SH-SY5Y cells. Furthermore, **1** showed good selectivity and moderate affinity for CB₁ receptors [19].

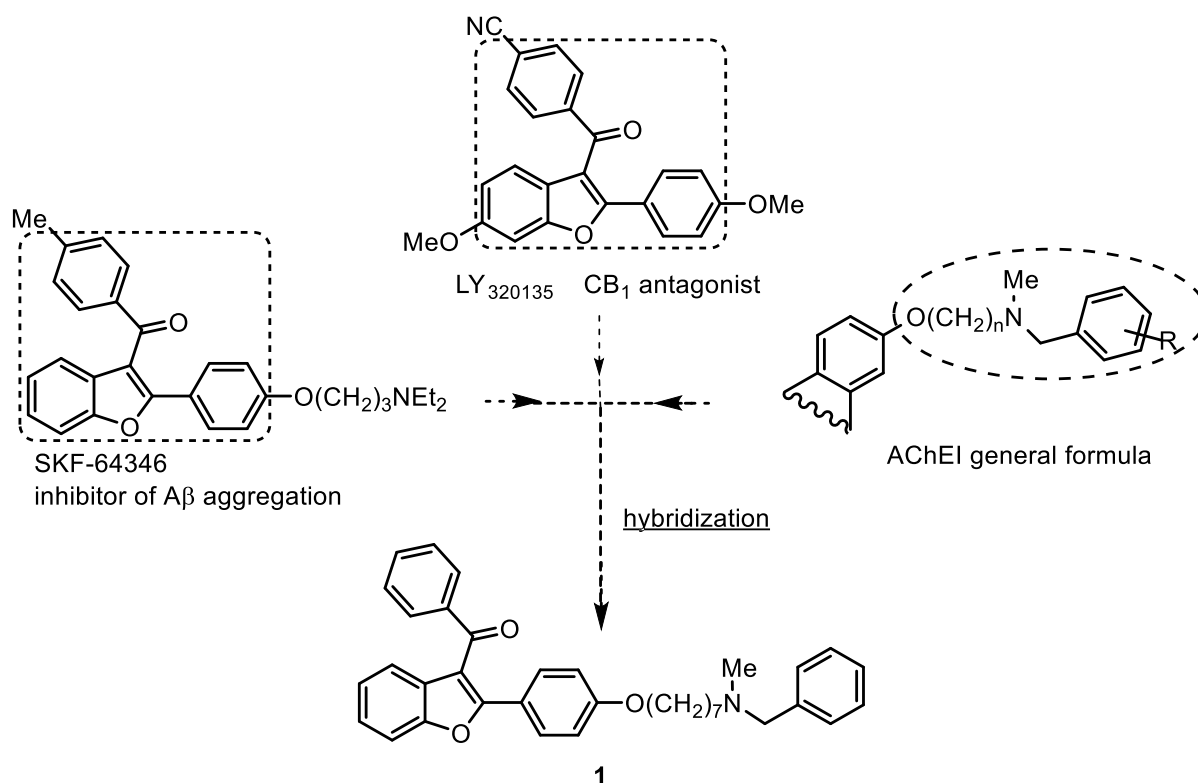


Figure 1. Design of the lead compound **1**.

As a follow-up of our previous studies, and aiming at optimizing/improving the biological activities and further exploring the chemical space of the selected targets, here we report the design, synthesis and biological evaluation of a new series of 2-arylbenzofuran derivatives, based on the structure of lead compound **1** (Figure 2).

At first, the *N*-methyl-*N*-benzylamine alkoxy side chain was moved from ring A to ring B and the polymethylene alkoxy spacer was varied to determine its optimal length (**2-5**). This linker chain was also removed, leading to a direct linking of mono or di-alkylated amines to ring B (**6-18**). Finally, taking into account that click chemistry has found increasing applications in drug discovery, this approach was exploited to achieve compound **19**, by introducing a substituted triazole.

This item was downloaded from IRIS Università di Bologna (<https://cris.unibo.it/>)

When citing, please refer to the published version.

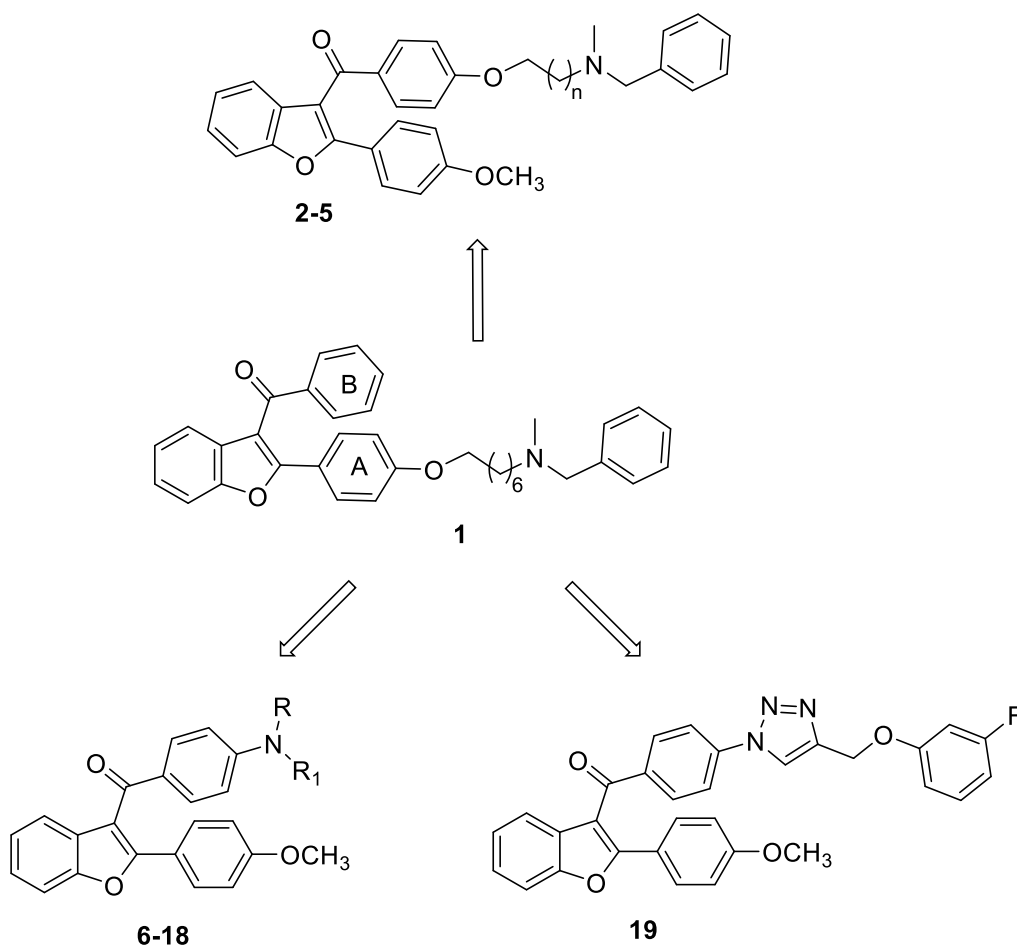


Figure 2. Design strategy for compounds **2-19**.

In summary, a small library of eighteen new derivatives, whose structures are collected in Tables 1 and 2, was synthesized. All compounds were assayed for their biological activities towards selected targets involved in AD, namely human AChE and BuChE, and CB receptors. After a preliminary screening, the two most promising compounds (**8** and **10**) were assessed for their neuroprotective activity and for their ability to modulate the microglial phenotype switch from the pro-inflammatory M1 to the anti-inflammatory M2 phenotype.

This item was downloaded from IRIS Università di Bologna (<https://cris.unibo.it/>)

When citing, please refer to the published version.

2. Results

2.1. Chemistry

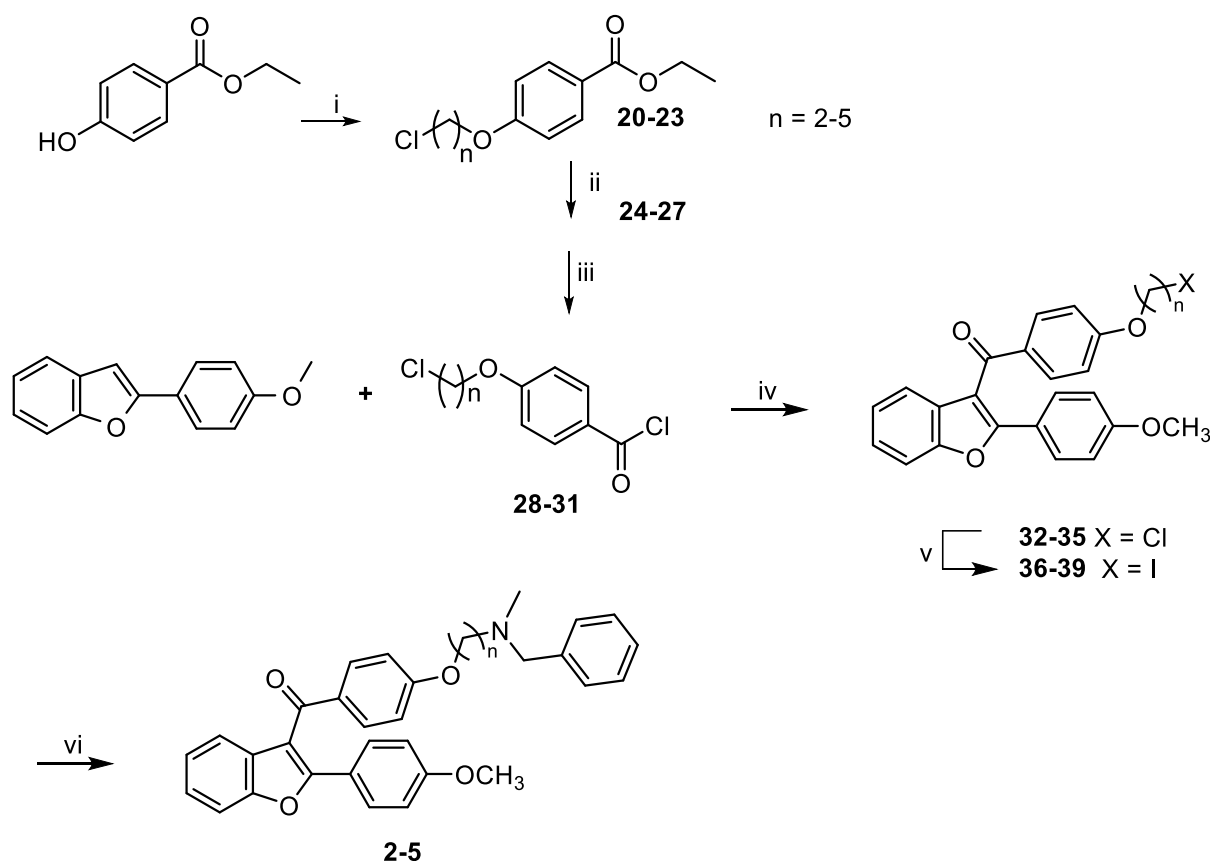
According to Scheme 1, 2-(4-methoxyphenyl)benzofuran underwent Friedel Craft acylation, using acyl chlorides **28-31** in order to obtain compounds **32-35**, which were treated with NaI affording the corresponding iodo analogues (**36-39**), more reactive species for the following nucleophilic substitution, that was accomplished by refluxing compounds **36-39** with *N*-methyl-*N*-benzylamine, and TEA in toluene to give the desired compounds **2-5**.

The key acyl intermediates **28-31** were prepared via alkylation of the hydroxyl group of the 4-hydroxyethyl benzoate in basic conditions with 1-bromo- ω -chloroalkanes in order to obtain **20-23**, which *via* saponification with potassium hydroxide led to compounds **24-27**. These carboxylic acids were then converted into the corresponding acyl chlorides (**28-31**) by treatment with thionyl chloride.

Scheme 1. Synthesis of compounds **2-5**.^a

This item was downloaded from IRIS Università di Bologna (<https://cris.unibo.it/>)

When citing, please refer to the published version.



Reagents and conditions: i) $\text{Br}(\text{CH}_2)_n\text{Cl}$, K_2CO_3 , acetone, reflux; ii) KOH , EtOH , reflux; iii) SOCl_2 , reflux; iv) SnCl_4 , DCM , 0°C , r.t.; v) NaI , MeCOEt , reflux; vi) N -methyl- N -benzylamine, TEA , toluene, reflux.

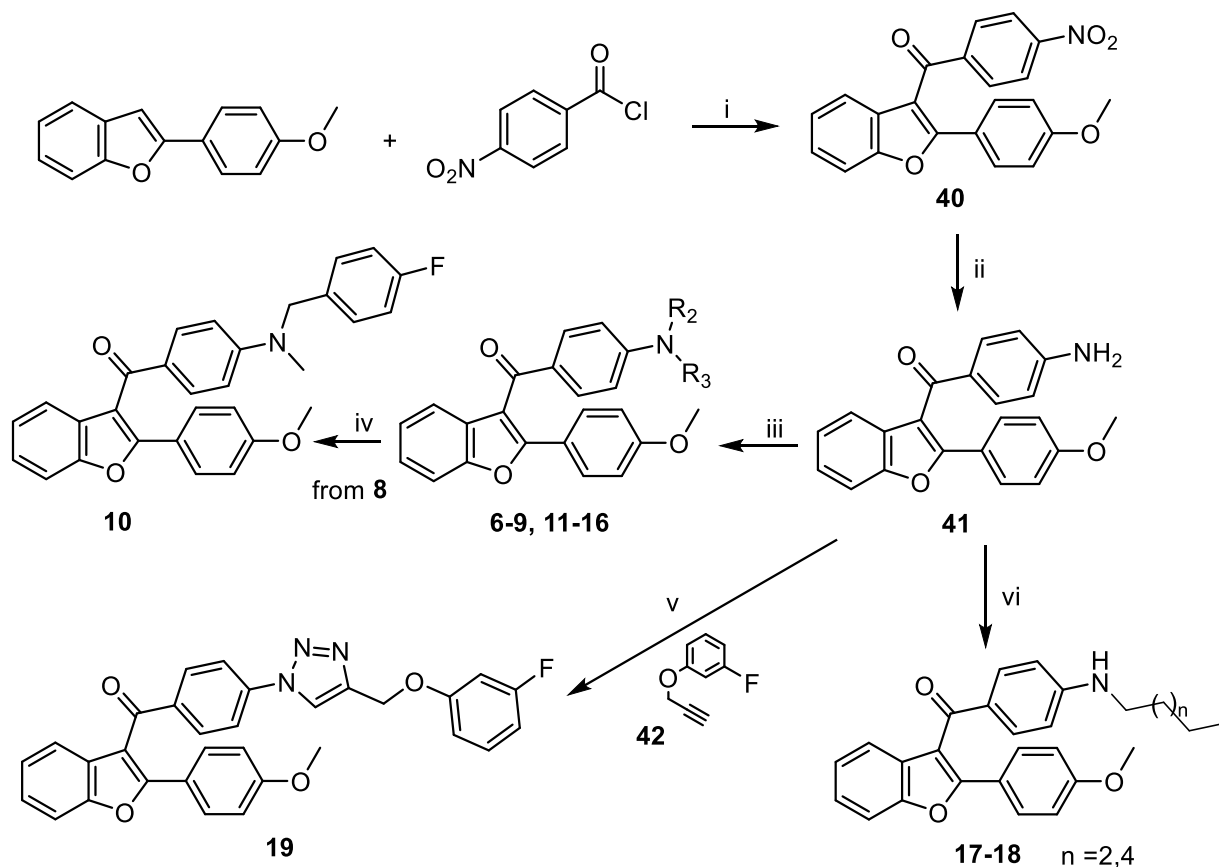
When the Friedel Craft acylation was carried out with 4-nitrobenzoylchloride, compound **40** was obtained (Scheme 2). The nitro group was reduced to the corresponding amine **41** by refluxing with SnCl_2 ; this intermediate was then reacted with the selected benzyl bromide in the presence of KI and K_2CO_3 and in a microwave oven, to obtain the mono- and di-alkylated compounds (**6-9**, **11-16**). Compound **8** was methylated in a biphasic mixture of DCM/NaOH 50% using CH_3I in presence of tetrabutylammonium hydrogensulfate obtaining **10**; with the same procedure, using the appropriate

This item was downloaded from IRIS Università di Bologna (<https://cris.unibo.it/>)

When citing, please refer to the published version.

bromoalkane, alkylated compounds **17-18** were obtained from **41**. Compound **19** was prepared via a click reaction, CuI-catalyzed Huisgen 1,3-dipolar cycloaddition, combining **41** with the alkyne **42** in the presence of tert-butyl nitrite and azidotrimethylsilane (TMSN₃) in CH₃CN.

Scheme 2. Synthesis of compounds **6-19**.^a



Reagents and conditions: i) SnCl₄, DCM, 0 °C; ii) SnCl₂, EtOH, reflux; iii) selected benzyl bromide, KI, K₂CO₃, CH₃CN, 110 °C, 150W, MW; iv) CH₃I, tetrabutylammonium hydrogensulfate, DCM/NaOH 50%, r.t.; v) tert-butyl nitrite, TMSN₃, CH₃CN, r.t.; vi) 1-bromopentane or 1-bromoheptane, tetrabutylammonium hydrogensulfate, DCM/NaOH 50%, r.t.

2.2. Biological evaluation

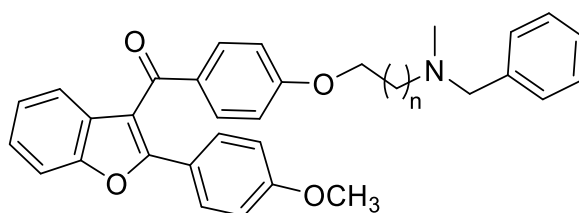
This item was downloaded from IRIS Università di Bologna (<https://cris.unibo.it/>)

When citing, please refer to the published version.

2.2.1. Cholinesterase inhibition

The evaluation of the inhibitory activity toward human recombinant AChE (*hAChE*) and BuChE from human serum (*hBuChE*) was performed according to Ellman's method [20], and the inhibitory potencies, expressed as IC₅₀ values, are listed in Tables 1 and 2, together with that of anticholinesterase drug galanthamine.

Table 1. Inhibitory activities exerted by compounds **2-5** and the reference compound galanthamine towards human AChE and BuChE expressed as IC₅₀ values.



Compd	n	% inhib. <i>hAChE</i>	% inhib. <i>hBuChE</i>	IC ₅₀ <i>hBuChE</i> (μM) ^b
		[I] = 25 μM ^a	[I] = 25 μM ^a	
1		IC ₅₀ = 40.7 ± 3.5 ^c		38.1 ± 2.2 ^c
2	1	n.a.	65.0 ± 1.0	14.0 ± 0.9
3	2	n.a.	35.0 ± 2.7	135 ± 6
4	3	n.a.	35.2 ± 0.7	219 ± 94
5	4	11.6 ± 3.6	> 90	1.09 ± 0.07

This item was downloaded from IRIS Università di Bologna (<https://cris.unibo.it/>)

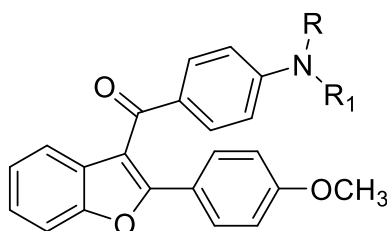
When citing, please refer to the published version.

Galantamine	-	>90% ^d	54.2 ± 1.8	20.7 ± 1.5
--------------------	---	-------------------	------------	------------

^a % inhibition of human recombinant AChE or BuChE from human serum at 25 μM. % inhibition are expressed as mean ± standard error of the mean (SEM) of at least two experiments, each performed in duplicate. ^bIC₅₀ inhibitory values for inhibition of *h*BuChE are expressed as mean ± standard error of the mean (SEM) of at least two experiments, each performed in duplicate. ^cData from ref [15], involving the same experimental conditions. ^dIC₅₀(*h*AChE) = (2.77 ± 0.13) μM. n.a.: = % inhibition not significant (<10%) at the tested concentration.

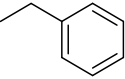
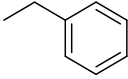
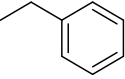
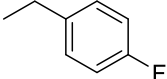
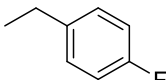
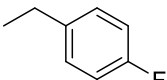
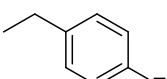
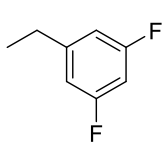
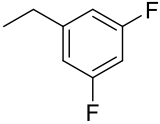
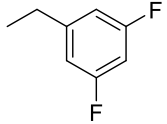
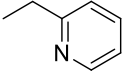
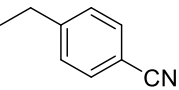
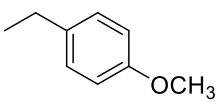
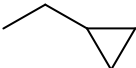

With respect to the lead compound **1**, all the new derivatives lost their *h*AChE inhibitory activity, while some of them showed an increased inhibition of *h*BuChE, thus displaying a different selectivity profile. In particular, in the first series (**2-5**, Table 1), the shift of the *N*-methyl-*N*-benzylamine alkoxy side chain from ring A to ring B, while making the compounds inactive on *h*AChE, led to an increased potency toward *h*BuChE, being compound **5** a good and selective BuChE inhibitor (35 folds more active than **1** and 19 folds more active than galanthamine). Moreover, a correlation between potency and side chain length was observed, being the two- and five-methylene linkers (compounds **2** and **5**) considerably more favorable than three or four (compounds **3** and **4**).

Table 2. Inhibitory activities exerted by of compounds **6-19** and the reference compound galanthamine on human AChE and BuChE expressed as IC₅₀ values.



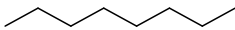
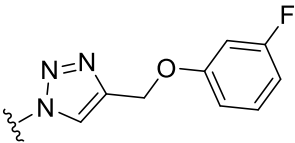
This item was downloaded from IRIS Università di Bologna (<https://cris.unibo.it/>)

When citing, please refer to the published version.

Compd	R	R ₁	% inhib <i>h</i> AChE [I] = 25 μM ^a	% inhib <i>h</i> BuChE [I] = 25 μM ^a	IC ₅₀ BuChE (μM) ^b
6	H		n.a.	n.a.	n.d.
7			n.a.	30.9 ± 1.8	n.d.
8	H		n.a.	60.8 ± 1.1	13.4 ± 0.5
9			19.4 ± 2.38	75.0 ± 1.4	6.03 ± 0.74
10	CH ₃		n.a.	n.a.	n.d.
11	H		n.a.	n.a.	n.d.
12			n.a.	67.0 ± 0.1	11.7 ± 0.4
13	H		n.a.	15.3 ± 1.2	n.d.
14	H		16.5 ± 3.2	n.a.	n.d.
15	H		n.a.	n.a.	n.d.
16	H		n.a.	22.4 ± 1.5	n.d.
17	H		n.a.	72.2 ± 0.2	3.90 ± 0.90

This item was downloaded from IRIS Università di Bologna (<https://cris.unibo.it/>)

When citing, please refer to the published version.

18	H		n.a.	30.2 ± 2.9	n.d.
19			n.a.	n.a.	n.d.
Galantamine	-		>90%	54.2 ± 1.8	20.7 ± 1.5

^a % inhibition of human recombinant AChE or BuChE from human serum at 25 μ M. % inhibition are expressed as mean \pm standard error of the mean (SEM) of at least two experiments, each performed in duplicate. ^bIC₅₀ inhibitory values for inhibition of *h*BuChE. IC₅₀ values are expressed as mean \pm standard error of the mean (SEM) of at least two experiments, each performed in duplicate. n.a. = % inhibition not significant (<10%) at the tested concentration. n.d. = not determined.

In the second series (**6-19**, Table 2), only compounds **8**, **9**, **12** and **17** showed inhibitory activity on *h*BuChE in the micromolar range, being compound **17** the most potent within this series.

Noteworthy, these four compounds exhibited higher potency with respect to the lead compound **1**, which showed balanced, albeit low, potency on both cholinesterases. Due to their weak potency, clear structure-activity relationships (SARs) cannot be drawn for this subset of derivatives.

2.2.2. CB₁ and CB₂ receptors affinity

The binding affinities of compounds **2-19** at human recombinant CB₁ and CB₂ receptors were determined by a competition assay using a high affinity ligand, i.e. [³H]-CP-55,940. Results are reported in Table 3, together with the K_i (inhibition constant) value for compound **1** and for SR144528 as reference CB₂ receptor ligand.

This item was downloaded from IRIS Università di Bologna (<https://cris.unibo.it/>)

When citing, please refer to the published version.

In the first series (compounds **2-5**, Table 3), moving the *N*-methyl-*N*-benzylamine alkoxy side chain from ring A to ring B caused a loss of selectivity for CB₁ with respect to the appreciable result observed for lead **1**. In particular, the affinity for the CB₁ receptor decreased with the increase of the linker length (compounds **2-5**); furthermore, while **1** was CB₁-selective, the new hybrids bearing the shorter linker chain (2- or 3-methylene units linker, derivatives **2** and **3**, respectively) showed a slightly higher affinity for CB₂ receptors, while compounds **4** and **5**, bearing a longer spacer chain, were CB₁-selective. Thus, a proper chain length seems to be a relevant feature for the modulation of both activity and selectivity. In this respect, compound **3** showed the highest potency and selectivity (4-fold) towards CB₂.

Removal of the spacer chain, with the direct linking of alkylated amines to ring B, led to improved affinity for the CB₂ receptor, which seemed to be favorably modulated by the aryl substituent. Indeed, the introduction of a fluorine atom in *para* position induced a 10-fold increase in the potency (**8** vs **6**, K_i = 20 nM and 170 nM, respectively). A similar behavior was observed with the introduction of a CN group (**14**), while a methoxy function (**15**) led to a 50-fold reduction of activity. The bioisosteric substitution of the benzene with a pyridine (**13**) reduced potency by an order of magnitude, while the cyclopropyl analogue **16** was equipotent to **6**. With the substitution of the benzene ring with a heptamethylene alkyl chain, as in compound **18**, a 2.5-fold decrease in potency was observed. Conversely, a shorter pentamethylene chain (**17**) led to a 2.5-fold increase in activity. Di-alkylated amines bound to B ring showed a loss of potency (**12**) or a decrease in activity with respect to mono-alkylated derivatives (**9** vs **8**, and, to a lesser extent, **7** vs **6**). Noteworthy, the introduction of a small methyl group on compound **8**, allowed achieving the most potent compound of the series (**10**, K_i = 2.7 nM, 600 folds more active than SR144528).

This item was downloaded from IRIS Università di Bologna (<https://cris.unibo.it/>)

When citing, please refer to the published version.

In the second series, appreciable CB₁ affinity in the nanomolar range was observed for derivatives **8**, **10**, **14**, **16-18**. The introduction of a F (**8**) or a CN (**14**) substituent on the aromatic ring seemed to be favorable for receptor binding. The introduction of a cyclopropyl (**16**) and, mainly, a short five-methylene unit chain (**17**, K_i = 80 nM) led to a significant increase in activity. Once again, the most potent compound in this series was the methyl di-alkylated **10** (K_i = 20 nM), which proved to be a potent ligand for both receptors, with a selectivity index (SI) towards CB₂ of 7.4. In this respect, the removal of a methyl group yielding the mono-alkylated **8**, led to increased selectivity up to 39 folds (CB₂ over CB₁). Nevertheless, the most selective compound of the series was **14**, again a mono alkylated derivative, bearing a CN group on the benzene ring. Compound **14** showed a SI of two orders of magnitude (SI = 130) towards CB₂. The length of the side chain also affected selectivity: the presence of a 5-unit chain led to a comparable potency at both receptors (**17**, K_i = 80 and 70 nM), while a 7-methylene chain allowed to better discriminate between the two receptor subtypes, i.e. derivative **18** showed a 4-fold higher affinity for CB₂.

Finally, compound **19**, bearing a substituted triazole, was inactive at both CB₁ and CB₂ receptors.

Table 3. Effect of compounds **2-19** and of reference compound SR144528 on [³H]-CP55940 binding to the human recombinant CB₁ and CB₂ receptors.

Compd	IC ₅₀ on CB ₁ μM m ± SD	K _i on CB ₁ μM m ± SD	IC ₅₀ on CB ₂ μM m ± SD	K _i on CB ₂ μM m ± SD	SI ^a
1	0.79 ^b	0.32 ^b	>10 ^b	>10 ^b	

This item was downloaded from IRIS Università di Bologna (<https://cris.unibo.it/>)

When citing, please refer to the published version.

2	1.52 ± 0.28	0.43 ± 0.08	2.63 ± 0.33	0.69 ± 0.09	0.6
3	2.06 ± 0.20	0.50 ± 0.05	0.44 ± 0.09	0.12 ± 0.02	4.2
4	3.52 ± 0.52	0.86 ± 0.13	>10	>10	
5	7.20 ± 1.47	1.76 ± 0.36	>10	>10	
6	>10	>10	0.66 ± 0.04	0.17 ± 0.01	> 59
7	>10	>10	3.64 ± 0.24	0.92 ± 0.06	> 11
8	3.21 ± 1.37	0.78 ± 0.33	0.07 ± 0.001	0.02 ± 0.00	39
9	>10	>10	1.65 ± 0.15	0.43 ± 0.04	> 23
10	0.08 ± 0.03	0.02 ± 0.01	0.01 ± 0.001	0.0027 ± 0.0000	7.4
11	>10	>10	1.15 ± 0.23	0.30 ± 0.06	> 33
12	>10	>10	>10	>10	
13	>10	>10	5.09 ± 1.45	1.34 ± 0.38	> 7.5
14	9.12 ± 0.17	2.60 ± 0.05	0.09 ± 0.00	0.02 ± 0.00	130
15	>10	>10	3.86 ± 0.46	1.02 ± 0.12	> 10
16	1.67 ± 0.59	0.47 ± 0.17	0.41 ± 0.06	0.11 ± 0.01	4.3
17	0.30 ± 0.07	0.08 ± 0.02	0.26 ± 0.001	0.07 ± 0.00	1.1
18	5.84 ± 2.32	1.66 ± 0.66	1.54 ± 0.29	0.41 ± 0.08	4
19	>10	>10	>10	>10	

This item was downloaded from IRIS Università di Bologna (<https://cris.unibo.it/>)

When citing, please refer to the published version.

SR144	541.9 ± 103.03	116.8 ± 22.20	7.16 ± 1.83	1.82 ± 0.46	64.2
528					

^aSI: selectivity index for CB₂, calculated as Ki(CB₁)/Ki(CB₂); ^bData from ref [19]

2.2.3. CB₂ receptor functional activity

The most potent CB₂ ligand **10** was further evaluated to assess its capability of activating CB₂ receptor in a functional assay. A cAMP Hunter™ assay using an enzyme fragment complementation chemiluminescent detection kit was performed to assess whether compound **10** could modulate intracellular cAMP levels in NKH-477-stimulated CHO cells overexpressing the human recombinant CB₂ receptor. In the selected assay conditions, **10** induced an increase of cAMP levels following stimulation with NKH-477 (a water-soluble analogue of forskolin), suggesting an inverse agonist behavior (Figure 3).

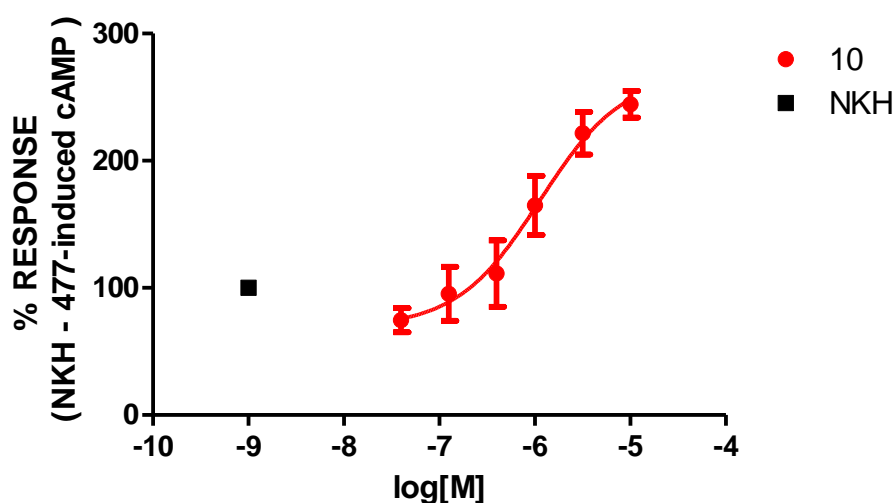


Figure 3. Concentration-response curve showing the effect of increasing concentrations of compound **10** on NKH-477-induced cAMP levels in stable CHO cells expressing the human CB₂ receptor. Data, reported as mean ± SEM of three independent experiments, were normalized to the

This item was downloaded from IRIS Università di Bologna (<https://cris.unibo.it/>)

When citing, please refer to the published version.

maximal and minimal response observed considering the NKH-477 stimulus alone as 100% of the response.

To confirm this hypothesis, **10** was tested in the presence of a previously determined EC₈₀ CB₂-agonist challenge (JWH133, 4μM). Accordingly, we found that **10** dose-dependently displaced the challenge of JWH133 and increased cAMP levels following the NKH-477 stimulus (Figure 4).

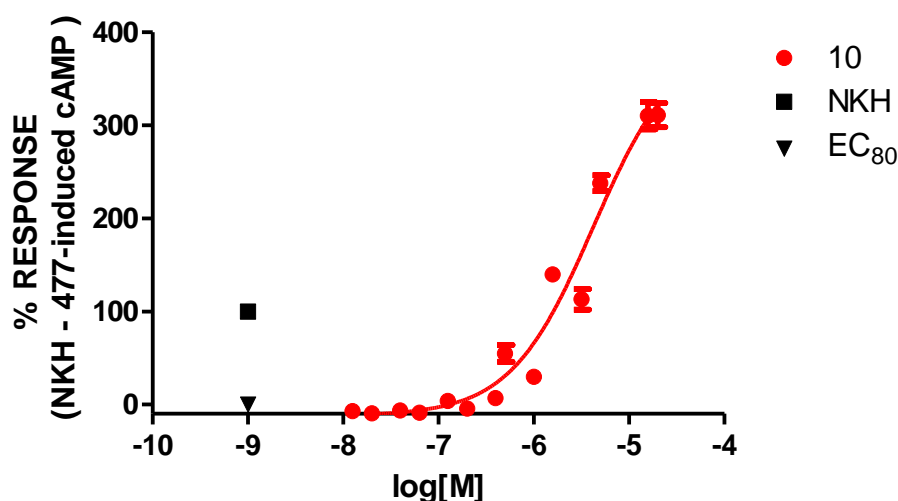


Figure 4. Concentration-response curve showing the effect of increasing concentrations of compound **10** on NKH-477-induced cAMP levels and in presence of an EC₈₀ CB₂-ligand challenge (4μM of JWH-133), in stable CHO cells expressing the human CB₂.

2.2.4. Neuroprotective activity

The cytotoxicity of compounds **8** and **10** was evaluated in human SH-SY5Y neuroblastoma cells using the MTT assay. After 24 h of treatment with different concentrations of compounds **8** or **10** (1.25 – 40 μM) residual cell viability was assessed. Data showed that concentrations up to 5 μM of both derivatives did not affect neuronal cell viability (data not shown). Therefore, we selected a

This item was downloaded from IRIS Università di Bologna (<https://cris.unibo.it/>)

When citing, please refer to the published version.

range of not cytotoxic concentrations (0.625 – 5 μ M) to investigate the neuroprotective activity of compounds **8** and **10** against A β ₁₋₄₂ oligomer (OA β ₁₋₄₂)-induced neurotoxicity in SH-SY5Y cells. The neuroprotective activity was evaluated after 4 h of treatment with OA β ₁₋₄₂ (10 μ M) in the presence of compounds **8** or **10** using the MTT formazan exocytosis assay. Only the treatment with compound **8** significantly counteracted, in a dose-dependent manner, the neurotoxicity induced by OA β ₁₋₄₂ (Figure 5).

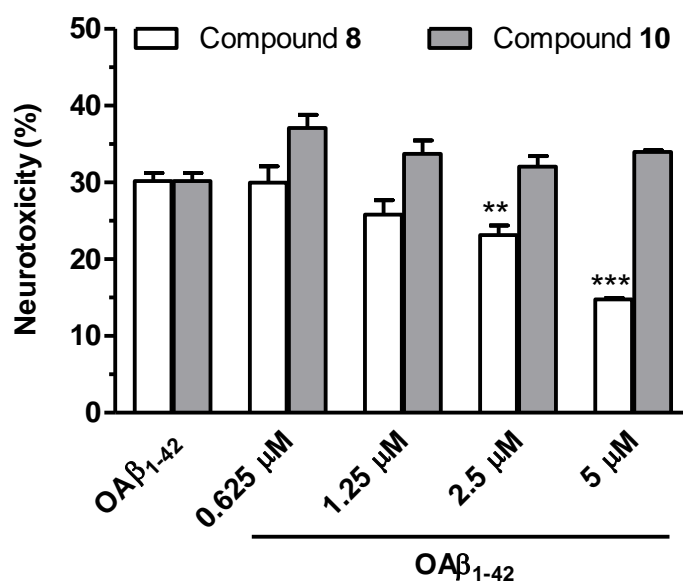


Figure 5. Compound **8**, unlike compound **10**, counteracts the neurotoxicity induced by OA β ₁₋₄₂ in SH-SY5Y cells. The neurotoxicity was evaluated using the MTT formazan exocytosis assay as described in the materials and methods section. Data are expressed as percentages of neurotoxicity and reported as mean \pm SEM of at least three independent experiments (** p < 0.01 and *** p < 0.001 versus cells treated with OA β ₁₋₄₂ at two-way ANOVA with Bonferroni post hoc test).

2.2.5. Activation of Microglia

The possible immunomodulatory effects of compounds **8**, **10** and of the lead **1** were evaluated by analyzing the expression of inducible nitric oxide synthase (iNOS), which is widely considered a

marker of M1 neurotoxic microglia, and of the triggering receptor expressed on myeloid cells 2 (TREM2), a marker of M2 neuroprotective microglia, in immortalized murine N9 cells, after exposure to lipopolysaccharide (LPS; 100 ng/mL), a widely–used pro-inflammatory stimulus (Figure 6 and 7) [21-22].

After treatment with compounds **8** and **10**, reduction of the M1 marker iNOS was observed with a maximum effect at 5 μ M (inhibition: 83% for compound **8**; 60% for compound **10**), with no concomitant decrease in TREM2 expression (Figure 6). This suggests an immunomodulatory effect for both compounds.

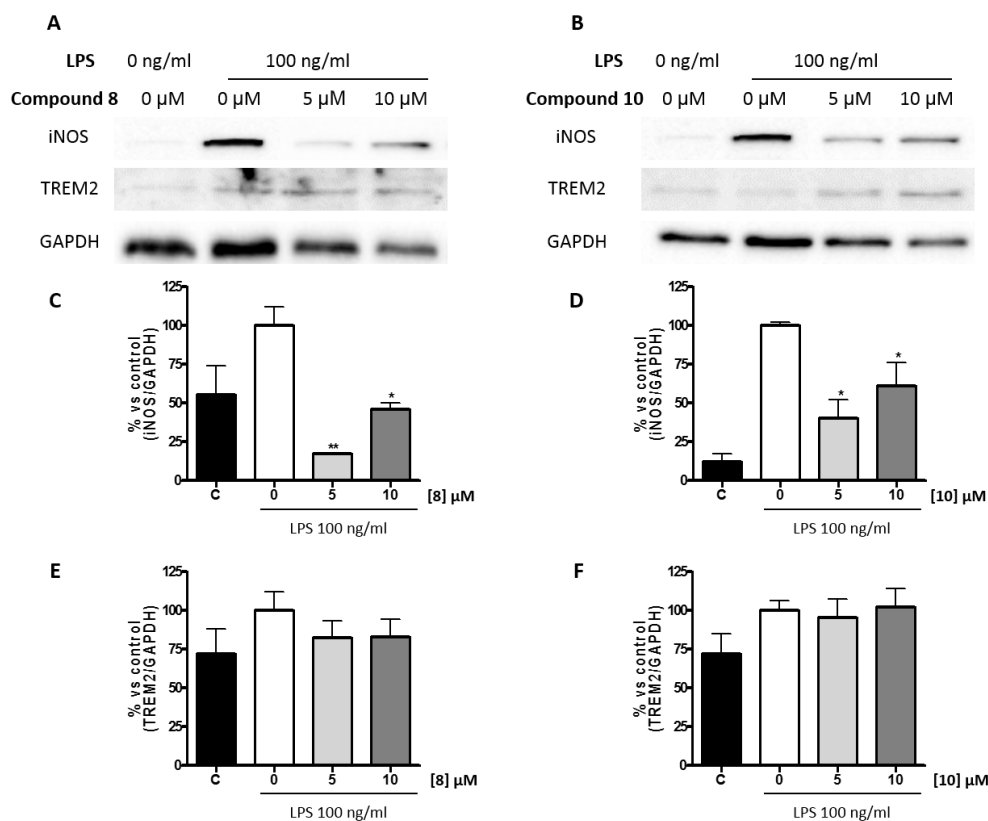


Figure 6. Western blot analysis of iNOS and TREM2 expression as microglial polarization markers (A, B) and their relative densitometries (C, D, E, F) to evaluate the immunomodulatory effects of

This item was downloaded from IRIS Università di Bologna (<https://cris.unibo.it/>)

When citing, please refer to the published version.

compounds **8** and **10** in N9 cell line. GAPDH was used as loading control. Densitometric results are expressed as percentage of LPS only and are the mean \pm SE of three different experiments.

* $p < 0.05$, ** $p < 0.01$ compared to LPS condition; Bonferroni's test after ANOVA.

Regarding the lead compound **1**, a toxic effect was observed at the lowest assayed concentration (5 μ M). Indeed, as reported in Figure 7, glyceraldehyde 6-phosphate dehydrogenase (GAPDH, loading control) expression appeared considerably reduced, suggesting the occurrence of cell death.

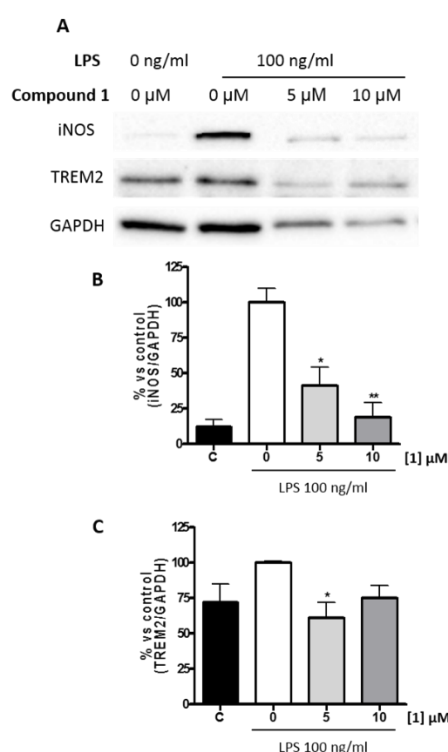


Figure 7. Western blot analysis of iNOS and TREM2 expression as microglial polarization markers (A) and their relative densitometries (B, C) to evaluate the immunomodulatory effects of compound **1** in N9 cell line.

2.2.6. Molecular docking studies

This item was downloaded from IRIS Università di Bologna (<https://cris.unibo.it/>)

When citing, please refer to the published version.

Finally, being compound **8** also endowed with a significant *h*BuChE inhibitory activity, a molecular docking simulation was performed using Autodock Vina software [23], in order to explore the binding mode of this derivative toward *h*BuChE and provide more insights into the possible interactions with the enzyme. We applied docking studies based on the available crystal structure of the *h*BuChE complexed with tacrine (PDB ID: 4BDS) with a grid box of sufficient size to cover whole protein for docking.

The docking simulation of **8** discloses that this compound can be efficiently accommodated inside the active site gorge with a molecular docking score of -10.7 kcal/mol (Figure 8a). Three-dimensional (3D) and two-dimensional (2D) representations of the most energetically profitable pose of compound **8** docked into the active site of BuChE were given in Figures 8b and 8c.

The complex of protein with the best-docked pose of inhibitor showed that the benzofuran moiety is located at the entrance of the active-site gorge with both side chains oriented deep inside the gorge.

The phenyl ring aromaticity clearly plays a dominant role in stabilizing inhibitor binding. The *p*-F-benzyl moiety is oriented toward the bottom of the active site and it binds in the CAS region of the enzyme establishing strong π - π stacking interactions with Trp82 and His438 of the catalytic-triad.

The methoxy-phenyl ring forms π - π T-shaped interactions with Phe329 in the acyl-binding pocket of the enzyme. The amino-phenyl ring forms π - π stacking interaction with Tyr332 of the PAS.

Apart from these π - π interactions, a hydrogen bond was established between the oxygen atom of the methoxy group and the hydroxyl group of Ser198 of the catalytic triad.

Notably, the F atom in the phenyl ring interacted with amino acids to form halogen interactions. F atom held Gly115 and Glu197 at one binding site resulting in the presence of $F\cdots C=O$ and $F\cdots O$ interactions (Figures 8b and 8c). These residues were near and in the sub-site known as “oxyanion

This item was downloaded from IRIS Università di Bologna (<https://cris.unibo.it/>)

When citing, please refer to the published version.

hole” formed by Gly115, Gly116 and Gly117 and having an essential role in catalysis. These non-covalent interactions were fairly strong, with the bond distances being around 3.60 Å.

In conclusion, docking studies revealed the capability of compound **8** to bind to CAS and PAS of *h*BuChE and induce its inhibitory effect.

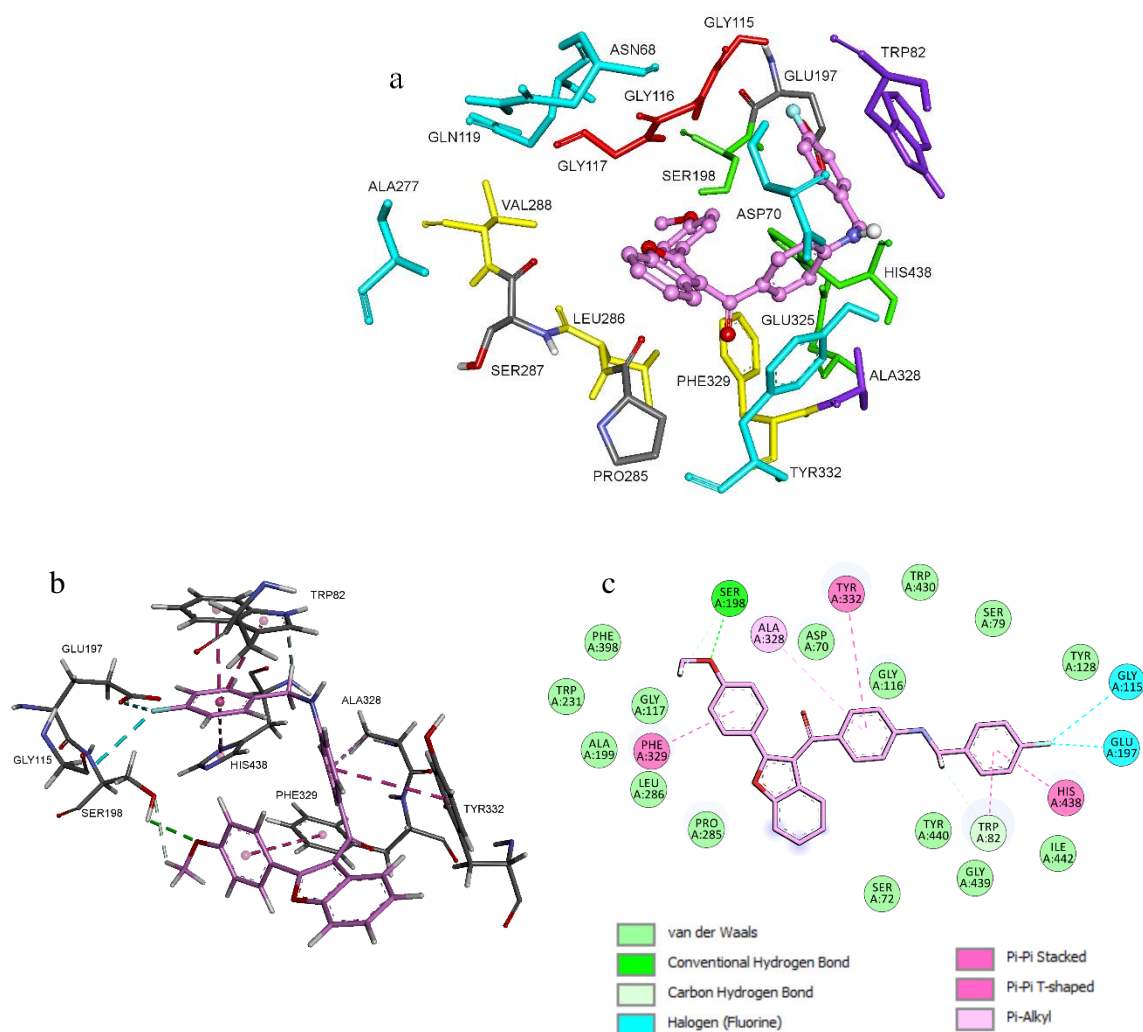


Figure 8. Docking poses of compound **8** inside gorge cavity of *h*BuChE. a) Compound **8** is coloured in pink. Different subsites of the active site were differently coloured: catalytically anionic site (CAS) in green, oxyanion hole (OH) in red, choline binding site in violet (CBS), acyl binding pocket (ABP) in yellow, and peripheral site (PAS) in blue. b) 3D representation of the amino acids

This item was downloaded from IRIS Università di Bologna (<https://cris.unibo.it/>)

When citing, please refer to the published version.

in the binding site interacting with the ligand **8**. c) 2D representation of the amino acids in the binding site interacting with the ligand **8**.

3. Discussion

In this paper the potential multitarget profile of two series of benzofuran derivatives, focused on the structure of the previously reported lead compound **1**, was assessed. From the results, some considerations can be drawn.

In the first series (compounds **2-5**), moving the side chain from A to B ring allowed achieving selectivity towards *h*BuChE, while affinity for the two cannabinoid receptors was modulated by the length of the linker. In particular, compound **5**, with a 5-methylene chain, showed a balanced effect on the two targets, with a good inhibitory activity on *h*BuChE and appreciable affinity and selectivity for CB₁ receptors. This finding is of particular interest since BuChE has recently gained a renewed interest as a therapeutic target in AD, since changes in its activity along disease progression were highlighted. Indeed, the brain levels of BuChE are un-altered or progressively increased during AD progression, while AChE activity declines [24]. On the other hand, CB₁ antagonists caused improvement in memory in several preclinical models of cognitive impairment [25-26].

In the second series (**6-18**), the linker chain was removed, leading to a direct binding of mono or dialkylated amines to B ring. Again, from a multitarget point of view, derivatives **8**, **9** and **17** emerged as good *h*BuChE inhibitors and CB receptors ligands. In particular, compound **9** was endowed with a peculiar selectivity for CB₂ receptors. Notably, derivatives **8** (*p*-F-benzyl alkylated) and **9** (bis-*p*-F-benzyl alkylated) contain fluorine atoms. Organofluorine compounds have recently been claimed as one of the most promising class of drug candidates in medicinal chemistry [27-29]. Indeed,

This item was downloaded from IRIS Università di Bologna (<https://cris.unibo.it/>)

When citing, please refer to the published version.

fluorine and fluoro-functional groups can be of crucial importance in affecting potency and pharmacokinetic properties of bioactive compounds, as the unique nature of fluorine strongly impacts on the chemical properties of the products [27]. On the other hand, **17** contains a *n*-pentyl alkyl chain, able to mimic the side chain of classical natural and synthetic cannabinoid ligands.

Aiming at evaluating the possible involvement of CB₂ receptor in neuroinflammation, compound **8**, showing affinity for both receptors, although with a preference for CB₂ receptor (SI = 39), and **10**, endowed with the highest CB₂ binding affinity (K_i = 2.7 nM) were selected for further studies.

First of all, the most potent CB₂ ligand (**10**) was evaluated to assess its capability of functionally activating the CB₂ receptor. Under the functional assay conditions, this compound induced an increase of cAMP levels, suggesting an inverse agonist behavior.

The compounds were then evaluated to establish their neuroprotective activity against OAβ₁₋₄₂-induced neurotoxicity in SH-SY5Y cells. Inflammation, indeed, represents a consistent feature in AD brain, and mounting evidence suggests that a neuroinflammatory response may be implicated in disease development. Insoluble deposits of Aβ are strong candidates for initiating the inflammatory response, whereas activated microglia and astrocytes could trigger a self-propagating neuroinflammatory process resulting in brain damage. Treatment with compound **8** significantly counteracted, in a dose-dependent manner, the OAβ₁₋₄₂-induced neurotoxicity while **10** was inactive. Recent studies have reported that both CB₁ and CB₂ receptors are expressed in SH-SY5Y cells, but have also highlighted the lack of a functional role for CB receptor agonists in response to Aβ exposure in these cells [30]. Therefore, the neuroprotective activity exerted by **8** may be due to its putative mode of action, i.e., inverse agonist at CB₂ receptor, a property for which this compound proved to be 39 folds more selective than the inactive derivative **10**. However, it cannot be excluded at this stage that the neuroprotective activity of **8** could also result from a direct, non-

This item was downloaded from IRIS Università di Bologna (<https://cris.unibo.it/>)

When citing, please refer to the published version.

CB receptor-mediated, action on A β peptide. In this regard, we have previously demonstrated that the benzoyl group of compound **1** is crucial [15] for the interaction with the hydrophobic residues of A β peptide, such as Ile31, Ile32 and Met35, that are critical for both neurotoxicity and aggregation processes [31-32]. Indeed, the neuroprotective effects of benzofuran derivative **8**, but not **10**, carrying an additional secondary amino group, may be related to its ability to form further donor hydrogen bonds with the same amino acid residues of A β peptide.

Microglial cells represent the main immune cells of the brain and are widely considered a promising target to counteract neuroinflammatory diseases, including AD. In physiological conditions, they constantly survey the parenchyma, while in neuropathological conditions they become activated, and play different roles depending on the duration and the gravity of the insult. Indeed, at an early stage of the disease, in order to protect neurons and fight the pathology, microglia acquire a M2 phenotype; later, when the disease progresses and expands, a M1 phenotype develops, and these cells become neurotoxic, producing proinflammatory cytokines, and leading to neuroinflammation. For these reasons, immunomodulation, i.e. the shift of microglial cells from the neurotoxic M1 to neuroprotective M2 phenotype, is now widely considered a promising therapeutic approach to tackle neurodegenerative diseases, including AD [33-34].

Accumulating evidence indicates that cannabinoids can modulate the function of activated microglia and the release of cytotoxic factors [35]. It has been also shown that both CB receptors are expressed in microglia and astrocytes. Unlike the CB₁ receptor, which is constitutively expressed in microglia, the expression of CB₂ receptor is inducible and is modulated in response to the activation stage of microglia. In particular, CB₂ receptor levels undergo time-dependent changes during microglia activation, with the initial attempt to counteract inflammation [36-37].

This item was downloaded from IRIS Università di Bologna (<https://cris.unibo.it/>)

When citing, please refer to the published version.

Although much of the literature dealing with CB₂ immunomodulatory effects focuses on agonists [38], the *in vitro* studies involving microglia continue to produce inconsistent results on the role of CB₁ and CB₂ receptors in the action of cannabinoids. CB₂ agonists have raised great interest as candidates for neuroprotection in neurodegenerative disorders. By contrast, CB₂ antagonists/inverse agonists have been shown to be promising agents for immunomodulation therapies. Experimental studies have documented beneficial effects of the administration of CB₂ antagonists/inverse agonists in animal models of various inflammatory disorders, arthritic bone damage and experimental autoimmune encephalomyelitis [39]. Indeed, recent studies showed that CB₁ and CB₂ receptor antagonists can directly suppress iNOS induction and ROS generation in activated microglia, leading to a feasible neuroprotective outcome [40]. Moreover, the beneficial effect of SMM-189, a potent and selective CB₂ inverse agonist, in a mild traumatic brain injury model, suggested a possible anti-inflammatory activity, due to its ability of reducing the M1 and increasing the M2 phenotype of human and murine microglia *in vitro* [41]. Again, studies on the triaryl bis-sulphone, Sch.414319, also led to speculate that inverse agonists to the CB₂ receptor may serve as immune modulators [42]. Here we observed that compounds **8** and **10** were able to strongly reduce iNOS expression (an M1 marker) induced by LPS treatment, without changing TREM2 expression (an M2 marker). This indicates an immunomodulatory effect of both compounds even at low concentrations (5 μM). Notably, in the same experimental conditions, the lead compound **1**, a selective CB₁ ligand, was cytotoxic and induced cell death even at the lowest tested concentration, endorsing a potential key role of CB₂ receptors in immunomodulation.

In conclusion, compound **8** can face AD from several directions: it restores the cholinergic system by inhibiting BuChE, exerts a neuroprotective activity against Aβ₁₋₄₂ oligomers and is a potent CB receptor ligand, with 39-fold selectivity for CB₂. Compound **8** is able to exert an interesting

This item was downloaded from IRIS Università di Bologna (<https://cris.unibo.it/>)

When citing, please refer to the published version.

multifunctional action by combining anti-inflammatory and neuroprotective effects. In addition, since pro-inflammatory M1 microglia predominate in the advanced stage of AD and aggravate disease progression, compound **8** by interfering with the activation of M1, could be effective in halting lesion development.

Derivative **10** proved to be a potent CB₂ inverse agonist with promising immunomodulatory properties. Being the development of CB₂ receptor antagonists/inverse agonists still very limited, a clear estimation of the therapeutic impact of such a class of ligands must await initial clinical testing and data in humans. Indeed, the mechanisms whereby CB₂ modulation affects inflammation and immune cell function are complex and detailed pathways remain to be elucidated. CB₂ receptor antagonists are, therefore, useful tools for studying signaling pathways associated with CB₂ binding. In this respect, **10** could be considered as a new probe for a better understanding of the role of CB₂ receptors and to develop potential immunomodulating drugs acting *via* the endocannabinoid system.

4. EXPERIMENTAL

4.1. Chemistry

4.1.1. Chemistry. General Methods. Melting points were measured in glass capillary tubes on a Büchi SMP-20 apparatus and are uncorrected. Direct infusion ES-MS spectra were recorded on a Waters Micromass ZQ 4000 apparatus. NMR spectra were recorded in CDCl₃, unless differently indicated, on a Varian Gemini spectrometer at 400 MHz (¹H), 100 MHz (¹³C), and 376 MHz (¹⁹F). Chemical shifts (δ) are reported in parts per million (ppm) relative to tetramethylsilane (TMS) as internal standard, and spin multiplicities are given as s (singlet), d (doublet), t (triplet), m (multiplet)

This item was downloaded from IRIS Università di Bologna (<https://cris.unibo.it/>)

When citing, please refer to the published version.

or br (broad). Chromatographic separations were performed on silica gel columns (Kieselgel 40, 0.040-0.063 mm; Merck) by flash chromatography. Chemical purities of the tested compounds were determined by HPLC-MS which confirmed $\geq 95\%$ purity. (HPLC-MS: Agilent Technologies HP1100 instrument coupled with an Agilent Technologies MSD1100 single-quadrupole mass spectrometer; ZOBRAE-Eclipse XDB-C8 Agilent Technologies column; mobile phase: H₂O/CH₃CN, 0.4 mL/min, gradient from 30 to 80% CH₃CN in 8 min, 80% CH₃CN until 25 min; MS set up: full scan mode from $m/z = 50$ to 2600, scan time 0.1s in positive ion mode, ESI spray voltage 4500V, nitrogen gas 35psi, drying gas flow 11.5 mL/min, fragmentor voltage 20V). Compounds were named relying on the naming algorithm developed by CambridgeSoft Corporation and used in ChemDraw Professional 15.0.

4.1.2. (4-(2-(Benzyl(methyl)amino)ethoxy)phenyl)(2-(4-methoxyphenyl)benzofuran-3-

yl)methanone (2). A mixture of **36** (0.77 g, 1.56 mmol, 1.0 eq) and *N*-benzylmethylamine (0.38 g, 3.12 mmol, 2.0 eq) in toluene (28 mL) was stirred and refluxed for 60h, then, on cooling, the reaction mixture was washed three times with water (3 x 20 mL) and the organic layer was concentrated under *vacuum*. Compound **2** was purified via flash column chromatography (toluene/acetone 4:1). 0.48 g of **36** were obtained, yield 28 %, oil. ¹H NMR δ 7.84 (d, $J = 8.4$ Hz, 2H, Ar), 7.68 (d, $J = 8.4$ Hz, 2H, Ar), 7.54 (d, $J = 8.4$ Hz, 1H, Ar), 7.46 (d, $J = 7.6$ Hz, 1H, Ar), 7.28-7.13 (m, 4H, Ar), 7.25-7.21 (m, 3H, Ar), 6.81 (t, $J = 8.8$ Hz, 4H, Ar), 4.09 (t, $J = 6.0$ Hz, 2H, OCH₂), 3.77 (s, 3H, OCH₃), 3.61 (s, 2H, CH₂), 2.82 (t, $J = 6.0$ Hz, 2H, CH₂N), 2.33 (s, 3H, NCH₃). ¹³C NMR 190.9, 162.9, 160.6, 156.7, 153.5, 138.3, 132.2, 130.6, 129.6, 129.0, 128.8, 128.2, 127.1, 124.7, 123.5, 122.1, 121.1, 114.9, 114.2, 113.9, 110.9, 66.4, 62.6, 55.4, 55.2, 42.9. ES-MS m/z : 492 (M + H⁺), 514 (M + Na).

4.1.3. (4-(3-(Benzyl(methyl)amino)propoxy)phenyl)(2-(4-methoxyphenyl)benzofuran-3-yl)methanone (3).Compound **3** was obtained following the same procedure described for

compound **2** using **37** as starting material. Yield 58 %, yellow oil. ^1H NMR δ 7.86 (d, J = 8.8 Hz, 2H, Ar), 7.70 (d, J = 8.8 Hz, 2H, Ar), 7.55 (d, J = 8.0 Hz, 1H, Ar), 7.47 (d, J = 7.2 Hz, 1H, Ar), 7.32-7.15 (m, 7H, Ar), 6.81 (dd, J = 15.2 and 8.4 Hz, 4H, Ar), 4.03 (t, J = 6.2 Hz, 2H, OCH₂), 3.76 (s, 3H, OCH₃), 3.49 (s, 2H, CH₂), 2.51 (t, J = 6.4 Hz, 2H, CH₂N), 2.21 (s, 3H, NCH₃), 1.99-1.92 (m, 2H, CH₂). ^{13}C NMR δ 191.0, 163.3, 160.6, 156.6, 153.5, 139.0, 132.3, 130.5, 129.7, 128.8, 128.9, 128.2, 126.9, 124.8, 123.5, 122.2, 121.1, 115.0, 114.2, 114.0, 111.0, 66.3, 62.4, 55.2, 53.4, 42.2, 27.0. ES-MS m/z : 506 (M + H⁺), 528 (M + Na).

4.1.4. (4-(4-(Benzyl(methyl)amino)butoxy)phenyl)(2-(4-methoxyphenyl) benzofuran-3-yl)methanone (4).Compound **4** was obtained following the same procedure described for

compound **2** using **38** as starting material. Yield 68 %, yellow oil. ^1H NMR δ 7.85 (d, J = 8.8 Hz, 2H, Ar), 7.70 (d, J = 9.2 Hz, 2H, Ar), 7.53 (d, J = 8.4 Hz, 1H, Ar), 7.46 (d, J = 7.6 Hz, 1H, Ar), 7.30-7.13 (m, 7H, Ar), 6.82-6.76 (dd, J = 13.2 and 9.2 Hz, 4H, Ar), 3.92 (t, J = 6.4 Hz, 2H, OCH₂), 3.74 (s, 3H, OCH₃), 3.46 (s, 2H, CH₂), 2.38 (t, J = 7.2 Hz, 2H, CH₂N), 2.17 (s, 3H, NCH₃), 1.82-1.75 (m, 2H, CH₂), 1.68-1.61 (m, 2H, CH₂). ^{13}C NMR δ 190.9, 163.3, 160.7, 156.7, 153.5, 139.2, 132.3, 130.5, 129.7, 129.0, 128.2, 126.9, 125.3, 124.8, 123.5, 122.2, 121.1, 115.1, 114.2, 114.0, 111.0, 68.0, 62.4, 56.7, 55.3, 42.2, 26.8, 23.7. ES-MS m/z : 520 (M + H⁺), 542 (M + Na).

4.1.5. (4-((5-(Benzyl(methyl)amino)pentyl)oxy)phenyl)(2-(4-methoxyphenyl)benzofuran-3-yl)methanone (5).Compound **5** was obtained following the same procedure described for

compound **2** using **39** as starting material. Yield 58 %, dark yellow oil. ^1H NMR δ 7.86 (d, J = 8.8 Hz, 2H, Ar), 7.70 (d, J = 8.8 Hz, 2H, Ar), 7.55 (d, J = 8 Hz, 1H, Ar), 7.46 (d, J = 7.2 Hz, 1H, Ar), 7.32-7.19 (m, 7H, Ar), 6.81 (dd, J = 15.2 and 8.4 Hz, 4H, Ar), 3.96 (t, J = 6.4 Hz, 2H, OCH₂), 3.78

This item was downloaded from IRIS Università di Bologna (<https://cris.unibo.it/>)

When citing, please refer to the published version.

(s, 3H, OCH₃), 3.47 (s, 2H, CH₂), 2.37 (t, $J = 6.8$ Hz, 2H, CH₂N), 2.18 (s, 3H, NCH₃), 1.81-1.69 (m, 2H, CH₂), 1.57-1.53 (m, 2H, CH₂), 1.51-1.45 (m, 2H, CH₂). ¹³C NMR δ 191.0, 163.3, 160.6, 156.7, 153.5, 139.2, 132.3, 130.5, 129.7, 129.0, 128.9, 128.2, 126.9, 124.7, 123.5, 122.2, 121.1, 115.1, 114.2, 114.0, 111.0, 68.1, 62.4, 57.2, 55.3, 42.2, 29.0, 27.1, 23.8. ES-MS m/z : 534 (M + H⁺), 556 (M + Na).

4.1.6. (4-(Benzylamino)phenyl)(2-(4-methoxyphenyl)benzofuran-3-yl)methanone (6) and (4-(dibenzylamino)phenyl)(2-(4-methoxyphenyl)benzofuran-3-yl)methanone (7). To a solution of **41** (0.10 g, 0.29 mmol, 3.0 eq) in acetonitrile (3 mL), benzylbromide (0.05 g, 0.29 mmol, 3.0 eq), KI (0.02 g, 0.10 mmol, 1.0 eq) and K₂CO₃ (0.02 g, 0.10 mmol, 1.0 eq) were added. The reaction was carried out with the microwave apparatus at 110 °C, 150W, for 10 min, then it was poured in water and extracted in DCM (3 x 10 mL). A crude reaction comprising compounds **6** and **7** was obtained that were then separated and purified *via* flash column chromatography, using petroleum ether/ethyl acetate 7:3 as eluent. 0.04 g of **6** and 0.10 g of **7** were obtained. Compound **6**: yield 32 %, yellow oil. ¹H NMR δ 7.77 (d, $J = 8.8$ Hz, 2H, Ar), 7.71 (d, $J = 8.4$ Hz, 2H, Ar), 7.51 (d, $J = 8.0$ Hz, 1H, Ar), 7.42 (d, $J = 7.6$ Hz, 1H, Ar), 7.35-7.27 (m, 6H, Ar), 7.18 (t, $J = 7.5$ Hz, 1H, Ar), 6.84 (d, $J = 8.4$ Hz, 2H, Ar), 6.50 (d, $J = 8.8$ Hz, 2H, Ar), 4.63 (br, 1H, NH), 4.35 (d, $J = 4.0$ Hz, 2H, CH₂), 3.79 (s, 3H, OCH₃). ¹³C NMR δ 190.4, 160.4, 155.4, 153.4, 152.3, 138.0, 132.7, 129.3, 129.2, 128.8, 127.6, 127.4, 127.1, 124.5, 123.3, 122.4, 121.0, 115.3, 113.9, 111.6, 110.9, 55.3, 47.5. ES-MS m/z : 434 (M + H⁺). Compound **7**: yield 66 %, yellow oil. ¹H NMR δ 7.77 (d, $J = 9.0$ Hz, 2H, Ar), 7.71 (d, $J = 8.4$ Hz, 2H, Ar), 7.51 (d, $J = 8.0$ Hz, 1H, Ar), 7.47 (d, $J = 7.6$ Hz, 1H, Ar), 7.33-7.16 (m, 11H, Ar), 6.85 (d, $J = 8.8$ Hz, 2H, Ar), 6.64 (d, $J = 8.8$ Hz, 2H, Ar), 4.67 (s, 4H, CH₂), 3.81 (s, 3H, OCH₃). ¹³C NMR δ 190.2, 160.3, 155.4, 153.3, 153.1, 137.0, 132.5, 129.3, 129.1,

128.7, 127.2, 126.2, 126.3, 124.5, 123.2, 122.4, 121.0, 115.4, 113.8, 111.2, 110.8, 55.2, 53.8. ES-MS m/z : 524 ($M + H^+$).

4.1.7. (4-((4-Fluorobenzyl)amino)phenyl)(2-(4-methoxyphenyl)benzofuran-3-yl)methanone (8)

and (4-(bis(4-fluorobenzyl)amino)phenyl)(2-(4-methoxyphenyl)benzofuran-3-yl)methanone

(9). Compounds **8** and **9** were obtained following the previous described procedure, using **41** and 4-

fluorobenzyl bromide as starting materials. Compound **8**: yield 38 %, yellow oil. 1H NMR δ 7.71 (d, $J = 8.8$ Hz, 2H, Ar), 7.66 (d, $J = 8.8$ Hz, 2H, Ar), 7.46 (d, $J = 8.4$ Hz, 1H, Ar), 7.38 (d, $J = 7.6$ Hz, 1H, Ar), 7.24-7.18 (m, 3H, Ar), 7.13 (t, $J = 7.2$ Hz, 1H, Ar), 6.95 (t, $J = 8.8$ Hz, 2H, Ar), 6.79 (d, $J = 8.4$ Hz, 2H, Ar), 6.44 (d, $J = 8.8$ Hz, 2H, Ar), 4.75 (br, 1H, NH), 4.27 (d, $J = 5.6$ Hz, 2H, CH₂), 3.74 (s, 3H, OCH₃). ^{13}C NMR δ 190.3, 163.3, 160.8, 160.4, 153.4, 152.6, 132.5, 129.4, 129.1, 128.1, 128.0, 126.7, 124.6, 123.3, 122.3, 121.0, 115.8, 115.6, 113.8, 111.3, 110.9, 55.3, 53.2. ES-MS m/z : 452 ($M + H^+$), 474 ($M + Na$). Compound **9**: yield 25 %, yellow oil. 1H NMR δ 7.70 (d, $J = 8.8$ Hz, 2H, Ar), 7.63 (d, $J = 8.8$ Hz, 2H, Ar), 7.45-7.39 (m, 4H, Ar), 7.22 (t, $J = 7.2$ Hz, 1H, Ar), 7.13 (t, $J = 7.6$ Hz, 1H, Ar), 7.06-7.03 (m, 4H, Ar), 6.94 (t, $J = 8.4$ Hz, 4H, Ar), 6.79 (d, $J = 8.8$ Hz, 2H, Ar), 6.56 (d, $J = 9.2$ Hz, 2H, Ar), 4.54 (s, 4H, CH₂), 3.75 (s, 3H, OCH₃). ^{13}C NMR δ 190.4, 163.2, 160.4, 153.4, 152.6, 132.5, 129.4, 129.0, 128.1, 128.0, 126.7, 124.6, 123.3, 122.4, 121.0, 115.8, 115.6, 113.8, 112.0, 111.3, 110.9, 55.3, 53.2. ES-MS m/z : 560 ($M + H^+$), 582 ($M + Na$).

4.1.8. (4-((4-Fluorobenzyl)(methyl)amino)phenyl)(2-(4-methoxyphenyl)benzofuran-3-

yl)methanone (10). A mixture of **8** (1.0 eq) and CH₃I (2.0 eq) was dissolved in a biphasic mixture of DCM/aq NaOH 50%, 1.5:1, then tetrabutylammonium hydrogensulfate (2.0 eq) was added and the reaction was stirred at r.t. for 4h. The organic layer was separated and washed with water, dried, and concentrated under reduced pressure to give the crude **10** that was purified *via* flash column chromatography, using petroleum ether/ethyl acetate 7:3 as eluent. 0.03 g of **10** as pure compound

This item was downloaded from IRIS Università di Bologna (<https://cris.unibo.it/>)

When citing, please refer to the published version.

were obtained, yield 14 %, yellow oil. ^1H NMR δ 7.82 (d, J = 9.0 Hz, 2H, Ar), 7.74 (d, J = 8.9 Hz, 2H, Ar), 7.54 (d, J = 8.2 Hz, 1H, Ar), 7.46 (d, J = 7.8 Hz, 1H, Ar), 7.31 (t, J = 7.2 Hz, 1H, Ar), 7.21 (t, J = 7.4 Hz, 1H, Ar), 7.12 (dd, J = 8.4 and 5.2 Hz, 2H, Ar), 7.01 (t, J = 8.6 Hz, 2H, Ar), 6.87 (d, J = 8.9 Hz, 2H, Ar), 6.62 (d, J = 9.0 Hz, 2H, Ar), 4.58 (s, 2H, CH_2), 3.82 (s, 3H, OCH_3), 3.09 (s, 3H, NCH_3). ^{13}C NMR δ 190.7, 160.4, 155.4, 153.4, 153.1, 133.0, 132.9, 132.5, 129.3, 129.2, 128.0, 127.9, 126.0, 124.5, 123.3, 122.4, 121.0, 115.7, 115.5, 115.4, 113.9, 110.9, 55.3, 55.2, 38.5. ^{19}F NMR δ -115.39--115.47 (m). ES-MS m/z : 466 ($\text{M} + \text{H}^+$), 488 ($\text{M} + \text{Na}$).

4.1.9. (4-((3,5-Difluorobenzyl)amino)phenyl)(2-(4-methoxyphenyl)benzofuran-3-yl)methanone (11) and (4-(bis(3,5-difluorobenzyl)amino)phenyl)-(2-(4-methoxyphenyl)benzofuran-3-yl)methanone (12). Compounds **11** and **12** were obtained following the same procedure described for compound **6** using **41** and 3,5-difluorobenzyl bromide as starting materials. Compound **11**: yield 73 %, yellow oil. ^1H NMR δ 7.76 (d, J = 8.4 Hz, 2H, Ar), 7.70 (d, J = 8.8 Hz, 2H, Ar), 7.51 (d, J = 8 Hz, 1H, Ar), 7.42 (d, J = 7.6 Hz, 1H, Ar), 7.30-7.24 (m, 1H, Ar), 7.18 (t, J = 7.4 Hz, 1H, Ar), 6.84-6.79 (m, 4H, Ar), 6.67 (t, J = 8.8 Hz, 1H, Ar), 6.46 (d, J = 8.8 Hz, 2H, Ar), 4.77 (br, 1H, NH), 4.35 (d, J = 6.0 Hz, 2H, CH_2), 3.78 (s, 3H, OCH_3). ^{13}C NMR δ 190.3, 164.6, 162.3, 160.5, 155.9, 153.4, 151.8, 141.2, 132.6, 129.4, 127.6, 124.6, 123.4, 122.2, 121.0, 113.9, 111.4, 110.9, 109.2, 109.0, 103.0, 55.3, 46.7. ES-MS m/z : 470 ($\text{M} + \text{H}^+$). Compound **12**: yield 23 %, yellow oil. ^1H NMR δ 7.82 (d, J = 9.2 Hz, 2H, Ar), 7.72 (d, J = 8.8 Hz, 2H, Ar), 7.54 (d, J = 8.0 Hz, 1H, Ar), 7.49 (d, J = 7.6 Hz, 1H, Ar), 7.33-7.21 (m, 3H, Ar), 6.88 (d, J = 8.8 Hz, 2H, Ar), 6.75-6.66 (m, 5H, Ar), 6.60 (d, J = 9.2 Hz, 2H, Ar), 4.65 (s, 4H, CH_2), 3.82 (s, 3H, OCH_3). ^{13}C NMR δ 164.6, 162.1, 160.5, 155.7, 153.4, 151.7, 142.5, 132.6, 129.4, 129.1, 127.6, 124.6, 123.3, 122.3, 121.0, 115.2, 113.9, 111.8, 110.9, 109.8, 102.8, 55.3, 53.7. ES-MS m/z : 596 ($\text{M} + \text{H}^+$), 618 ($\text{M} + \text{Na}$).

4.1.10. (2-(4-Methoxyphenyl)benzofuran-3-yl)(4-((pyridin-2-ylmethyl)amino)phenyl)

methanone (13). Compound **13** was obtained following the same procedure described for compound **6** using **41** and 2-(bromomethyl)pyridine as starting materials. Yield 32 %, mp 56 °C. ¹H NMR δ 8.57 (d, *J* = 8.0 Hz, 1H, Ar), 7.74 (d, *J* = 8.8 Hz, 2H, Ar), 7.69-7.61 (m, 3H, Ar), 7.49 (d, *J* = 8.0 Hz, 1H, Ar), 7.40 (d, *J* = 8.0 Hz, 1H, Ar), 7.27-7.14 (m, 4H, Ar), 6.81 (d, *J* = 8.4 Hz, 2H, Ar), 6.51 (d, *J* = 8.4 Hz, 2H, Ar), 5.80 (br, 1H, NH), 4.45 (d, *J* = 5.6 Hz, 2H, OCH₂), 3.76 (s, 3H, OCH₃). ¹³C NMR δ 190.5, 178.1, 160.4, 156.9, 155.4, 153.4, 152.2, 149.0, 137.0, 132.7, 129.3, 129.2, 126.8, 124.5, 123.3, 122.5, 122.4, 121.9, 121.0, 115.3, 113.9, 111.7, 110.9, 55.3, 48.0. ES-MS *m/z*: 435 (M + H⁺), 457 (M + Na).

4.1.11. 4-(((4-(2-(4-Methoxyphenyl)benzofuran-3-carbonyl)phenyl)amino)methyl)benzonitrile

(14). Compound **14** was obtained following the same procedure described for compound **6** using **41** and 4-(bromomethyl)benzonitrile as starting materials. Yield 36 %, yellow oil. ¹H NMR δ 7.76 (d, *J* = 8.7 Hz, 2H, Ar), 7.70 (d, *J* = 8.9 Hz, 2H, Ar), 7.61 (d, *J* = 8.2 Hz, 2H, Ar), 7.54 (d, *J* = 8.2 Hz, 1H, Ar), 7.45 (d, *J* = 7.7 Hz, 1H, Ar), 7.39 (d, *J* = 8.1 Hz, 2H, Ar), 7.34-7.16 (m, 2H, Ar), 6.85 (d, *J* = 8.9 Hz, 2H, Ar), 6.46 (d, *J* = 8.8 Hz, 2H, Ar), 4.85 (br, 1H, NH), 4.45 (d, *J* = 6.0 Hz, 2H, CH₂), 3.82 (s, 3H, OCH₃). ¹³C NMR δ 190.4, 160.4, 155.7, 153.4, 151.7, 143.9, 132.6, 132.5, 129.4, 129.0, 129.1, 128.2, 127.6, 127.5, 125.3, 124.6, 123.3, 122.3, 121.0, 118.6, 115.1, 113.9, 111.8, 111.3, 110.9, 55.3, 46.9. ES-MS *m/z*: 459 (M + H⁺).

4.1.12. (4-((4-Methoxybenzyl)amino)phenyl)(2-(4-methoxyphenyl)benzofuran-3-yl) methanone

(15). Compound **15** was obtained following the same procedure described for compound **6** using **41** and 4-methoxybenzylchloride as starting materials. Yield 29 %, yellow oil. ¹H NMR δ 7.80 (d, *J* = 8.8 Hz, 2H, Ar), 7.74 (d, *J* = 8.8 Hz, 2H, Ar), 7.54 (d, *J* = 8.2 Hz, 1H, Ar), 7.45 (d, *J* = 7.7 Hz, 1H, Ar), 7.35-7.21 (m, 4H, Ar), 6.97-6.85 (m, 4H, Ar), 6.52 (d, *J* = 8.8 Hz, 2H, Ar), 4.47 (br, 1H, NH),

This item was downloaded from IRIS Università di Bologna (<https://cris.unibo.it/>)

When citing, please refer to the published version.

4.30 (s, 2H, CH₂), 3.81 (s, 3H, OCH₃), 3.80 (s, 3H, OCH₃). ¹³C NMR δ 192.8, 162.8, 161.5, 157.8, 155.8, 154.8, 135.1, 132.4, 131.7, 131.6, 131.2, 130.1, 129.4, 126.9, 125.7, 124.8, 123.4, 117.8, 116.6, 116.3, 114.0, 113.3, 57.7, 49.5. ES-MS *m/z*: 464 (M + H⁺).

4.1.13. (4-((Cyclopropylmethyl)amino)phenyl)(2-(4-methoxyphenyl)benzofuran-3-

yl)methanone (16). Compound **16** was obtained following the same procedure described for compound **6** using **41** and chloromethylcyclopropane as starting materials. Yield 26 %, yellow oil.

¹H NMR δ 7.77 (d, *J* = 8.6 Hz, 2H, Ar), 7.72 (d, *J* = 8.8 Hz, 2H, Ar), 7.51 (d, *J* = 8.4 Hz, 1H, Ar), 7.41 (d, *J* = 7.6 Hz, 1H, Ar), 7.29-7.18 (m, 2H, Ar), 6.84 (d, *J* = 8.4 Hz, 2H, Ar), 6.45 (d, *J* = 8.8 Hz, 2H, Ar), 4.37 (br, 1H, NH), 3.79 (s, 3H, OCH₃), 2.98 (d, *J* = 7.6 Hz, 2H, CH₂), 1.12-0.96 (m, 1H, CH), 0.56 (d, *J* = 7.2 Hz, 2H, CH₂), 0.24 (d, *J* = 4.8 Hz, 2H, CH₂). ¹³C NMR δ 190.3, 160.4, 155.3, 153.4, 152.6, 132.7, 132.6, 129.4, 129.3, 126.6, 124.5, 123.3, 122.4, 121.0, 115.4, 113.9, 111.3, 110.9, 55.3, 48.2, 10.6, 3.5. ES-MS *m/z*: 398 (M + H⁺), 420 (M + Na).

4.1.14. (2-(4-Methoxyphenyl)benzofuran-3-yl)(4-(pentylamino)phenyl)methanone (17).

Compound **17** was obtained following the same procedure described for compound **10** using **41** and 1-bromopentane as starting materials. Yield 42 %, oil. ¹H NMR δ 7.77 (d, *J* = 8.7 Hz, 2H, Ar), 7.72 (d, *J* = 8.9 Hz, 2H, Ar), 7.51 (d, *J* = 8.2 Hz, 1H, Ar), 7.42 (d, *J* = 7.7 Hz, 1H, Ar), 7.30-7.26 (m, 1H, Ar), 7.18 (t, *J* = 7.2 Hz, 1H, Ar), 6.84 (d, *J* = 8.9 Hz, 2H, Ar), 6.45 (d, *J* = 8.8 Hz, 2H, Ar), 4.20 (br, 1H, NH), 3.79 (s, 3H, OCH₃), 3.13 (t, *J* = 7.2 Hz, 2H, NCH₂), 1.62-1.57 (m, 4H, CH₂), 1.35-1.32 (m, 4H, CH₂), 0.90 (t, *J* = 6.8 Hz, 3H, CH₃). ¹³C NMR δ 190.3, 160.3, 155.2, 153.4, 153.3, 132.7, 129.3, 128.5, 126.5, 124.5, 123.2, 122.5, 121.0, 113.9, 111.3, 110.9, 55.3, 43.2, 29.1, 29.0, 22.4, 14.0. ES-MS *m/z*: 414 (M + H⁺).

4.1.15. (4-(Heptylamino)phenyl)(2-(4-methoxyphenyl)benzofuran-3-yl)methanone (18).

Compound **18** was obtained following the same procedure described for compound **6** using **41** and

This item was downloaded from IRIS Università di Bologna (<https://cris.unibo.it/>)

When citing, please refer to the published version.

1-bromoheptane as starting materials. Yield 31 %, oil. ^1H NMR δ 7.80-7.74 (m, 4H, Ar), 7.53 (d, J = 8.2 Hz, 1H, Ar), 7.44 (d, J = 7.8 Hz, 1H, Ar), 7.28 (t, J = 7.2 Hz, 1H, Ar), 7.18 (t, J = 7.6 Hz, 1H, Ar), 6.87 (d, J = 8.8 Hz, 2H, Ar), 6.47 (d, J = 8.7 Hz, 2H, Ar), 4.26 (br, 1H, NH), 3.81 (s, 3H, OCH₃), 3.17-3.12 (m, 2H, NCH₂), 1.62-1.58 (m, 2H, CH₂), 1.44-1.23 (m, 8H, CH₂), 0.87 (t, J = 6.4 Hz, 3H, CH₃). ^{13}C NMR δ 190.3, 160.4, 155.2, 153.4, 152.8, 132.7, 131.5, 129.2, 126.5, 124.5, 123.2, 122.5, 121.0, 115.4, 113.9, 113.8, 111.3, 110.9, 55.3, 43.3, 31.7, 29.7, 29.3, 27.0, 22.5, 14.0. ES-MS m/z : 442 ($\text{M} + \text{H}^+$).

4.1.16. (4-(4-((3-Fluorophenoxy)methyl)-1H-1,2,3-triazol-1-yl) phenyl)(2-(4-methoxyphenyl)benzofuran-3-yl)methanone (19). To a solution cooled to 0 °C of **41** (0.38 g, 1.11 mmol, 1.0 eq) in acetonitrile (14 mL), *tert*-butyl nitrite (0.17 g, 1.66 mmol, 1.5 eq) and TMSN₃ (0.15 g, 1.33 mmol, 1.2 eq) were added and the reaction was stirred at r.t. for 2h. Then, **42** (0.25 g, 1.66 mmol, 1.5 eq) and a solution of CuSO₄ (0.02 g, 0.11 mmol, 1/10 eq) and sodium ascorbate (0.11 g, 0.55 mmol, 0.5 eq) in water (2.05 mL) were added dropwise to the reaction flask. The mixture was stirred for 10h. The reaction was quenched with water and the organic compound was extracted with ethyl acetate (3 x 20 mL). Compound **19** was purified *via* flash column chromatography, using petroleum ether/ethyl acetate 3:1 as eluent to obtain 0.10 g of **19** as neat compound. Yield 17 %, oil. ^1H NMR δ 8.07 (s, 1H, Ar), 7.97 (d, J = 8.6 Hz, 2H, Ar), 7.72 (d, J = 8.6 Hz, 2H, Ar), 7.62-7.55 (m, 4H, Ar), 7.37 (t, J = 7.6 Hz, 1H, Ar), 7.33-7.21 (m, 2H, Ar), 6.81-6.77 (m, 3H, Ar), 6.74-6.68 (m, 2H, Ar), 5.26 (s, 2H, CH₂), 3.76 (s, 3H, OCH₃). ^{13}C NMR δ 190.6, 161.1, 158.9, 153.7, 144.9, 139.6, 138.1, 131.5, 130.5, 130.4, 130.3, 128.3, 125.2, 124.0, 121.7, 121.2, 120.7, 119.9, 114.4, 114.0, 111.2, 110.3, 108.4, 108.2, 102.8, 102.6, 62.1, 55.3. ^{19}F NMR δ -111.11 – -111.23 (m). ES-MS m/z : 520 ($\text{M} + \text{H}^+$), 542 ($\text{M} + \text{Na}$).

4.1.17. Ethyl 4-(2-chloroethoxy)benzoate (20). To a solution of 4-hydroxybenzoate (1.00 g, 6.02 mmol, 1.0 eq) in acetone (25 mL), 1-bromo-2-chloroethane (1.29 g, 9.036 mmol, 1.5 eq) and K_2CO_3 (2.49 g, 3.0 eq) were added. The reaction was refluxed and stirred for 10h, then it was hot filtered and concentrated under *vacuum*. The obtained crude **20** was purified *via* flash column chromatography, mobile phase toluene to give 1.60 g of neat compound as colorless oil, yield 86 %. 1H NMR δ 8.02 (d, $J = 9.2$ Hz, 2H), 6.95 (d, $J = 9.2$ Hz, 2H), 4.39-4.33 (m, 2H), 4.29 (t, $J = 5.4$ Hz, 2H), 3.85 (t, $J = 5.8$ Hz, 2H), 1.39 (t, $J = 7.2$ Hz, 3H).

4.1.18. Ethyl 4-(3-chloropropoxy)benzoate (21). Compound **21** was obtained following the same procedure described for compound **20** using 1-bromo-3-chloropropane as starting material. Colorless oil, yield 96 %. 1H NMR δ 8.02 (d, $J = 9.2$ Hz, 2H), 6.94 (d, $J = 8.4$ Hz, 2H), 4.38-4.33 (m, 2H), 4.19 (t, $J = 5.8$ Hz, 2H), 3.76 (t, $J = 6.4$ Hz, 2H), 2.56-2.30 (m, 2H), 1.39 (t, $J = 7.2$ Hz, 3H).

4.1.19. Ethyl 4-(4-chlorobutoxy)benzoate (22). Compound **22** was obtained following the same procedure described for compound **20** using 1-bromo-4-chlorobutane as starting material. Oil, yield 91 %. 1H NMR δ 8.01 (d, $J = 8.4$ Hz, 2H), 6.92 (d, $J = 8.8$ Hz, 2H), 4.38-4.33 (m, 2H), 4.08 (t, $J = 6.2$ Hz, 2H), 3.64 (t, $J = 5.6$ Hz, 2H), 2.00-1.98 (m, 4H), 1.39 (t, $J = 7.2$ Hz, 3H).

4.1.20. Ethyl 4-((5-chloropentyl)oxy)benzoate (23). Compound **23** was obtained following the same procedure described for compound **20** using 1-bromo-5-chlorobutane as starting material. Colorless oil, yield 98 %. 1H NMR δ 7.99 (d, $J = 8.8$ Hz, 2H), 6.91 (d, $J = 9.2$ Hz, 2H), 4.37-4.32 (m, 2H), 4.02 (t, $J = 6.2$ Hz, 2H), 3.56 (t, $J = 6.2$ Hz, 2H), 1.89-1.80 (m, 4H), 1.67-1.61 (m, 2H), 1.38 (t, $J = 7.2$ Hz, 3H).

4.1.21. 4-(2-Chloroethoxy)benzoic acid (24). To a solution of **20** (1.33 g, 5.85 mmol, 1 eq) in ethanol (40 mL), a solution of KOH (0.49 g, 8.78 mmol, 1.5 eq) in H₂O (2 mL) was added and the mixture was stirred and refluxed for 3h. The ethanol was evaporated under *vacuum*, then a 50% aqueous solution of HCl (20 mL) was added to the reaction mixture. A white solid precipitate was formed and filtered, obtaining **24** (1.37 g, yield 92 %, mp 176-178 °C). ¹H NMR 8.03 (d, *J* = 9.2 Hz, 2H), 6.95 (d, *J* = 8.8 Hz, 2H), 4.35 (t, *J* = 5.8 Hz, 2H), 3.91 (t, *J* = 6.2 Hz, 2H).

4.1.22. 4-(3-Chloropropoxy)benzoic acid (25). Compound **25** was obtained following the same procedure described for compound **24**, using **21** as starting material. Yield 87 %, mp 102 °C. ¹H NMR δ 8.04 (d, *J* = 9.2 Hz, 2H), 6.94 (d, *J* = 8.8 Hz, 2H), 4.17 (t, *J* = 5.8 Hz, 2H), 3.74 (t, *J* = 6.2 Hz, 2H), 2.25 (t, *J* = 6.0 Hz, 2H).

4.1.23. 4-(4-Chlorobutoxy)benzoic acid (26). Compound **26** was obtained following the same procedure described for compound **24** using **22** as starting material. Yield 92 %, mp 113 °C. ¹H NMR δ 8.05 (d, *J* = 8.8 Hz, 2H), 6.94 (d, *J* = 8.4 Hz, 2H), 4.09-4.06 (m, 2H), 3.63 (t, *J* = 6.0 Hz, 2H), 2.00-1.98 (m, 4H).

4.1.24. 4-((5-Chloropentyloxy)benzoic acid (27). Compound **27** was obtained following the same procedure described for compound **24** using **23** as starting material. Yield 97 %, mp 103-104 °C. ¹H NMR δ 8.06 (d, *J* = 9.2 Hz, 2H), 6.94 (d, *J* = 8.8 Hz, 2H), 4.06-4.02 (m, 2H), 3.58 (t, *J* = 6.6 Hz, 2H), 1.90-1.82 (m, 4H), 1.68-1.61 (m, 2H).

4.1.25. 4-(2-Chloroethoxy)benzoyl chloride (28). A mixture of **24** (1.12 g, 5.62 mmol) and SOCl₂ (18 mL) was stirred and refluxed for 5h, then the solvent was removed, obtaining **28** (1.40 g, yield 96 %, yellow oil). The compound was used for the next reaction without any further purification.

4.1.26. 4-(3-Chloropropoxy)benzoyl chloride (29). Compound **29** was obtained following the same procedure described for compound **28** using **25** as starting material. Yield 98 %, yellow oil.

4.1.27. 4-(4-Chlorobutoxy)benzoyl chloride (30). Compound **30** was obtained following the same procedure described for compound **28** using **26** as starting material. Yield 96 %, oil.

4.1.28. 4-((5-Chloropentyl)oxy)benzoyl chloride (31). Compound **31** was obtained following the same procedure described for compound **28** using **27** as starting material. Yield 96 %, yellow oil.

4.1.29. (4-(2-Chloroethoxy)phenyl)(2-(4-methoxyphenyl)benzofuran-3-yl)methanone (32). A mixture of 2-(4-methoxyphenyl)benzofuran (1.00 g, 4.49 mmol, 1 eq) and **28** (1.17 g, 5.38 mmol, 1.2 eq) in anhydrous DCM (30 mL), under nitrogen atmosphere, was cooled to 0 °C, then SnCl₄ (1.40 g, 5.38 mmol, 1.2 eq) was added dropwise. The mixture was stirred at r.t. overnight. The reaction was quenched with ice/water and stirred for 1 h. The organic layer was separated and the aqueous one was extracted with DCM (3 x 20 mL). The combined organic extracts were dried and concentrated under reduced pressure to afford **32** that was purified *via* flash column chromatography (petroleum ether/ethyl acetate 3:2). Yield: 61 %, oil. ¹H NMR δ 7.88 (d, *J* = 8.4 Hz, 2H), 7.69 (d, *J* = 8.8 Hz, 2H), 7.57 (d, *J* = 8.4 Hz, 1H), 7.49 (d, *J* = 8.0 Hz, 1H), 7.33 (t, *J* = 7.6 Hz, 1H), 7.23 (t, *J* = 7.4 Hz, 1H), 6.86 (d, *J* = 8.4 Hz, 4H), 4.24 (t, *J* = 5.6 Hz, 2H), 3.79 (s, 3H), 3.26 (t, *J* = 7.6 Hz, 2H).

4.1.30. (4-(3-Chloropropoxy)phenyl)(2-(4-methoxyphenyl)benzofuran-3-yl)methanone (33). Compound **33** was obtained following the same procedure described for compound **32** using **29** as starting material. Yield 40 %, yellow pale oil. ¹H NMR δ 7.88 (d, *J* = 9.2 Hz, 2H), 7.71 (d, *J* = 9.2 Hz, 2H), 7.55 (d, *J* = 8.0 Hz, 1H), 7.46 (d, *J* = 7.2 Hz, 1H), 7.30 (t, *J* = 7.6 Hz, 1H), 7.23 (t, *J* = 7.4

Hz, 1H), 6.85 (dd, $J = 8.8$ and 2.8 Hz, 4H), 4.15 (t, $J = 5.4$ Hz, 2H), 3.81 (s, 3H), 3.74 (t, $J = 6.4$ Hz, 2H), 2.31-2.20 (m, 2H).

4.1.31. (4-(4-Chlorobutoxy)phenyl)(2-(4-methoxyphenyl)benzofuran-3-yl)methanone (34).

Compound **34** was obtained following the same procedure described for compound **32** using **30** as starting material. Yield 71 %, oil. ^1H NMR δ 7.86 (d, $J = 9.2$ Hz, 2H), 7.69 (d, $J = 9.2$ Hz, 2H), 7.55 (d, $J = 8.0$ Hz, 1H), 7.46 (d, $J = 7.2$ Hz, 1H), 7.30 (t, $J = 7.6$ Hz, 1H), 7.23 (t, $J = 7.4$ Hz, 1H), 6.84-6.79 (m, 4H), 3.99 (t, $J = 5.4$ Hz, 2H), 3.78 (s, 3H), 3.59 (t, $J = 6.2$ Hz, 2H), 1.96-1.92 (m, 4H).

4.1.32. (4-((5-Chloropentyl)oxy)phenyl)(2-(4-methoxyphenyl)benzofuran-3-yl)methanone (35).

Compound **35** was obtained following the same procedure described for compound **32** using **31** as starting material. Yield 73 %, yellow oil. ^1H NMR δ 7.86 (d, $J = 9.2$ Hz, 2H), 7.69 (d, $J = 9.2$ Hz, 2H), 7.53 (d, $J = 8.4$ Hz, 1H), 7.46 (d, $J = 7.6$ Hz, 1H), 7.29 (t, $J = 7.8$ Hz, 1H), 7.21 (t, $J = 7.8$ Hz, 1H), 6.84-6.78 (m, 4H), 3.95 (t, $J = 6.4$ Hz, 2H), 3.76 (s, 3H), 3.52 (t, $J = 6.6$ Hz, 2H), 1.84-1.74 (m, 4H), 1.61-1.55 (m, 2H).

4.1.33. (4-(2-Iodoethoxy)phenyl)(2-(4-methoxyphenyl)benzofuran-3-yl)methanone (36). A

mixture of **32** (2.78 g, 5.58 mmol, 1.0 eq) and NaI (0.84 g, 5.58 mmol, 1.2 eq) in methyl ethyl ketone (70 mL) was stirred and refluxed for 5h. The solvent was removed under reduced pressure, then the crude was dissolved in DCM and washed with water (3 x 20 mL). The collected organic layers were concentrated under *vacuum*, obtaining **36** (2.38 g, yield 91 %, oil) that was used for the next reaction without any further purification.

4.1.34. (4-(3-Iodopropoxy)phenyl)(2-(4-methoxyphenyl)benzofuran-3-yl)methanone (37).

Compound **37** was obtained following the same procedure described for compound **36** using **33** as starting material. Yield 89 %, oil.

This item was downloaded from IRIS Università di Bologna (<https://cris.unibo.it/>)

When citing, please refer to the published version.

4.1.35. (4-(4-Iodobutoxy)phenyl)(2-(4-methoxyphenyl)benzofuran-3-yl)methanone (38).

Compound **38** was obtained following the same procedure described for compound **36** using **34** as starting material. Yield 93 %, oil.

4.1.36. (4-((5-Iodopentyl)oxy)phenyl)(2-(4-methoxyphenyl)benzofuran-3-yl)methanone (39).

Compound **39** was obtained following the same procedure described for compound **36** using **35** as starting material. Yield 79 %, oil.

4.1.37. (2-(4-Methoxyphenyl)benzofuran-3-yl)(4-nitrophenyl) methanone (40). A mixture of 2-(4-methoxyphenyl)benzofuran (1.10 g, 4.95 mmol, 1.0 eq) and 4-nitrobenzoyl chloride (1.10 g, 5.85 mmol, 1.2 eq) in anhydrous DCM (40 mL), under nitrogen atmosphere, was cooled at 0 °C, then SnCl₄ (1.55 g, 5.95 mmol, 1.2 eq) was added dropwise to the reaction flask. The reaction was stirred at r.t. for 10h, then it was quenched with ice and the organic compound was extracted with DCM (3 x 40 mL). 1.44 g of neat compound **40** were obtained. Yield 78 %, mp 146 °C. ¹H NMR δ 8.12 (d, *J* = 8.2 Hz, 2H), 7.89 (d, *J* = 8.2 Hz, 2H), 7.64 (d, *J* = 7.7 Hz, 1H), 7.59-7.48 (m, 3H), 7.37 (t, *J* = 7.6 Hz, 1H), 7.29 (t, *J* = 7.6 Hz, 1H), 6.77 (d, *J* = 8.2 Hz, 2H), 3.77 (s, 3H).

4.1.38. (4-Aminophenyl)(2-(4-methoxyphenyl)benzofuran-3-yl)methanone (41). To a solution of **40** (1.44 g, 3.86 mmol, 1.0 eq) in ethanol (100 mL), SnCl₂ (10.85 g, 48.25 mmol, 12.5 eq) was added and the reaction was refluxed for 2h. The mixture was cooled to r.t. and NaOH (40 mL) was added. The organic compound was extracted with ethyl acetate (3 x 40 mL). Compound **41** was purified *via* column flash chromatography, using petroleum ether/ethyl acetate 4:1 as eluent. 1.18 g of neat compound were obtained. Yield 89 %, mp 183 °C. ¹H NMR δ 7.77 (d, *J* = 8.6 Hz, 2H), 7.73 (d, *J* = 8.9 Hz, 2H), 7.55 (d, *J* = 8.2 Hz, 1H), 7.46 (d, *J* = 7.7 Hz, 1H), 7.31 (t, *J* = 8.3 Hz, 1H), 7.22 (t, *J* = 7.6 Hz, 1H), 6.87 (d, *J* = 8.9 Hz, 2H), 6.57 (d, *J* = 8.7 Hz, 2H), 4.13 (s, 2H), 3.82 (s, 3H).

This item was downloaded from IRIS Università di Bologna (<https://cris.unibo.it/>)

When citing, please refer to the published version.

4.1.39. 1-Fluoro-3-(prop-2-yn-1-yloxy)benzene (42). To a solution of 3-fluorophenol (1.00 g, 8.92 mmol, 1.0 eq) in acetone (100 mL), propargyl bromide (1.30 g, 10.70 mmol, 1.2 eq) and K₂CO₃ (1.00 g) were added. The reaction was stirred and refluxed for 8h, then it was hot filtered and concentrated under vacuum. Compound **42** was purified *via* flash column chromatography, using petroleum ether/ethyl acetate 9:1 as eluent. 1.03 g of neat compound **42** were obtained. Yield 77 %, oil. ¹H NMR δ 7.35-7.28 (m, 1H), 6.98-6.64 (m, 3H), 4.63 (d, *J* = 7.2 Hz, 2H), 2.58-2.48 (m, 1H).

4.2. Biological evaluation methods.

4.2.1. Inhibition of human AChE and BuChE. The inhibitory activity against human recombinant AChE was assessed using the method of Ellman *et al.* [20]. Initial rate assays were performed at 37 °C with a Jasco V-530 double beam Spectrophotometer (Jasco Europe, Italy). The rate of increase in the absorbance at 412 nm was followed for 180 s. AChE stock solution was prepared by dissolving human recombinant AChE lyophilized powder (Sigma-Aldrich, Italy) in 0.1 M phosphate buffer at pH = 8.0 containing 0.1% Triton X-100. BuChE stock solution was prepared by dissolving the lyophilized powder in an aqueous solution of gelatine 0.1%. Stock solutions of inhibitors (2.5 mM) were prepared in methanol and diluted in methanol. Stock solution (4.0 mM) of the reference compound galanthamine hydrobromide (Tocris Bioscience, UK) was prepared in bidistilled water and diluted in bidistilled water. Inhibitors were first screened at a single concentration (25 μM). Then, for compounds showing a percentage of inhibition higher than 35% at 25 μM, the IC₅₀ values were determined. For IC₅₀ assessment, five/six increasing concentrations of the inhibitor were evaluated, able to give an inhibition of the enzymatic activity in the range of 20-80%. The assay solution consisted of a 0.1 M phosphate buffer pH 8.0, with the addition of 340 μM (Ellman's reagent, 0.02 unit/mL of human recombinant AChE and 550 μM of substrate

This item was downloaded from IRIS Università di Bologna (<https://cris.unibo.it/>)

When citing, please refer to the published version.

(acetylthiocholine iodide or butyrylthiocholine iodide). 50 μ L aliquots of increasing concentration of the tested inhibitor (or methanol) were added to the assay solution and incubated with the enzyme for 20 min at 37 °C before the addition of the substrate. Blank solutions containing all components except AChE or BuChE were prepared in order to account for the non-enzymatic hydrolysis of the substrate. The reaction rates were compared and the percent inhibition due to the presence of inhibitor was calculated. Each concentration was analyzed in duplicate, and IC₅₀ values were determined graphically from log concentration–inhibition curves (GraphPad Prism 4.03 software, GraphPad Software Inc.). Two independent experiments were performed for the determination of each IC₅₀ value or % of inhibition at the screening level.

4.2.2. Competition Binding Assay. Membranes from HEK-293 cells over-expressing the respective human recombinant CB₁ receptor (B_{max} = 2.5 pmol/mg protein) and human recombinant CB₂ receptor (B_{max} = 4.7 pmol/mg protein) were incubated with [³H]-CP-55,940 (0.14 nM/K_d = 0.18 nM and 0.084 nM/K_d = 0.31 nM for CB₁R and CB₂R, respectively) as the high affinity ligand. Competition curves were performed as previously described [43]. Briefly, [³H]-CP-55,940 was displaced with increasing concentration of compounds (0.1 nM – 10 μ M). Nonspecific binding was defined by 10 μ M of WIN55,212-2 as the heterologous competitor (K_i values 9.2 nM and 2.1 nM, respectively, for CB₁ and CB₂ receptors). IC₅₀ values were determined for compounds showing >50% displacement at 10 μ M. All compounds were tested following the procedure described by the manufacturer (Perkin Elmer, Italy). Displacement curves were generated by incubating drugs with [³H]-CP-55,940 for 90 minutes at 30°C. K_i values were calculated by applying the Cheng-Prusoff equation to the IC₅₀ values (obtained by GraphPad) for the displacement of the bound radioligand by increasing concentrations of the test compound. Data represent mean values for of three independent

experiments performed in duplicate and are expressed as the average of IC_{50} and K_i (nM) \pm standard deviation.

4.2.3. Functional activity at CB₂ receptor in vitro. The cAMP Hunter™ assay enzyme fragment complementation chemiluminescent detection kit was used to characterize the functional activity in CB₂ receptor-expressing cell lines. Gi-coupled cAMP modulation was measured following the manufacturer's protocol (DiscoverX, Fremont, CA). Briefly, CHO-K1 cells overexpressing the human CB₂R were plated into a 96 well plate (30,000 cells/well), and incubated overnight at 37 °C, 5% CO₂. Media was aspirated and replaced with 30 μ L of assay buffer. Cells were incubated 30 min at 37 °C with 15 μ L of 3x dose-response solutions of samples prepared in presence of cell assay buffer containing a 3x of 25 μ M NKH-477 solution (a water soluble analogue of Forskolin) to stimulate adenylate cyclase and enhance basal cAMP levels. For those compounds showing an increase of cAMP levels, we further investigated their effect upon receptor activation by testing compounds in the presence of JWH-133, a selective agonist. Cells were pre-incubated with samples (15 min at 37 °C at 6x the final desired concentration) followed by 30 min incubation with JWH-133 agonist challenge at the EC₈₀ concentration (EC₈₀ = 4 μ M, previously determined in separate experiments) in presence of NKH-477 to stimulate adenylate cyclase and enhance cAMP levels. For all protocols, following stimulation, cell lysis and cAMP detection were performed as per the manufacturer's protocol. Luminescence measurements were measured carried out using a GloMax Multi Detection System (Promega, Italy). Data were reported as mean \pm SEM of three independent experiments conducted in triplicate and were normalized considering the NKH-477 stimulus alone as 100% of the response. The percentage of response was calculated using the following formula: % RESPONSE = 100% \times (1 – (RLU of test sample – RLU of NKH-477 positive control) / (RLU of vehicle – RLU of

This item was downloaded from IRIS Università di Bologna (<https://cris.unibo.it/>)

When citing, please refer to the published version.

NKH-477 positive control). The data were analysed using Prism software (GraphPad Software Inc, San Diego, CA).

4.2.4. Cell culture. Human neuronal (SH-SY5Y) cells were routinely grown in Dulbecco's modified Eagle's Medium supplemented with 10% fetal bovine serum, 2 mM L-glutamine, 50 U/mL penicillin and 50 µg/mL streptomycin at 37 °C in a humidified incubator with 5% CO₂.

4.2.5. Determination of cytotoxicity. Neuronal SH-SY5Y cells were seeded in a 96-well plate at 2×10^4 cells/well, incubated for 24 h and subsequently treated for 24 h with different concentrations of compounds **8** and **10** (1.25 – 40 µM). Cells viability, in terms of mitochondrial metabolic function, was evaluated by the reduction of 3-(4,5-dimethyl-2-thiazolyl)-2,5-diphenyl-2H-tetrazolium bromide (MTT) to its insoluble formazan, as previously described [44]. Briefly, the treatment medium was replaced with MTT in Hank's Balanced Salt Solution (HBSS) (0.5 mg/mL) for 2 h at 37 °C in 5% CO₂. After washing with HBSS, formazan crystals were dissolved in isopropanol. The amount of formazan was measured (570 nm, reference filter 690 nm) using a multilabel plate reader (VICTOR™ X3, PerkinElmer, Waltham, MA, USA). The quantity of formazan was directly proportional to the number of viable cells.

4.2.6. Aβ₁₋₄₂ oligomers preparation for the determination of neuroprotective activity. Aβ₁₋₄₂ peptide (AnaSpec, Fremont, CA, USA) was first dissolved in 1,1,1,3,3,3-hexafluoroisopropanol to 1 mg/mL, sonicated, incubated at room temperature for 24 h and lyophilized. The resulting unaggregated Aβ₁₋₄₂ peptide film was dissolved with DMSO and stored at –20 °C until use. The Aβ₁₋₄₂ peptide aggregation to oligomeric form was performed as previously described [45].

4.2.7. Determination of neuroprotective activity against Aβ₁₋₄₂ oligomers-induced neurotoxicity. Neuronal SH-SY5Y cells were seeded in a 96-well plate at 3×10^4 cells/well, incubated for 24 h and

This item was downloaded from IRIS Università di Bologna (<https://cris.unibo.it/>)

When citing, please refer to the published version.

subsequently treated for 4 h with A β ₁₋₄₂ oligomers (OA β ₁₋₄₂) (10 μ M) in the presence of compounds **8** or **10** (0.625 – 5.0 μ M). The neuroprotective activity, in terms of increase in intracellular formazan crystals, was evaluated using the MTT formazan exocytosis assay, as previously described [46]. Briefly, the treatment medium was replaced with MTT in HBSS (0.5 mg/mL) for 1 h at 37 °C in 5% CO₂. At the end of incubation, the intracellular MTT formazan was completely dissolved in 1% Tween 20. The amount of Tween 20-soluble MTT was measured at 570 nm (reference filter 690 nm) by using a multilabel plate reader (VICTOR™ X3, PerkinElmer). Data are expressed as percentages of neurotoxicity. Analyses were performed using Prism 5 software (GraphPad Software Inc, San Diego, CA, USA).

4.2.8. Immunomodulation activity on N9 immortalized cell line. N9, an immortalized murine microglia cell line, was used to investigate the immunomodulatory profile of selected compounds. Cells were grown on previously poly-L-lysine (10 μ g/mL, Sigma-Aldrich) coated Petri dishes at 37°C in a humidified atmosphere with 5% CO₂ in Dulbecco's Modified Eagle Medium High Glucose (DMEM) supplemented with 10% Fetal Bovine Serum (FBS), 1% Penicillin/Streptomycin solution and 2 mM L-glutamine (all reagents were from Aurogene). At confluence, cells were trypsinized and plated at a density of 2.5×10^5 cells/35 mm diameter Petri dishes. In order to activate microglial cells, cells were treated with the bacterial endotoxin lipopolysaccharide (LPS, 100 ng/mL, Sigma-Aldrich) in the presence or absence of the selected compounds at increasing concentrations (0, 5, 10 μ M) in DMEM medium without serum for 24 hours. Microglial cells were collected in 2X loading buffer (0.05 M Tris-HCl pH 6.8; 40 g/L sodium dodecyl sulfate; 20 mL/L glycerol; 2 g/L bromophenol blue and 0.02 M dithiothreitol; all from Sigma-Aldrich) for Western blot analysis.

4.2.9. Western Blot Analysis. Cells lysates were loaded onto 12.5 % sodium dodecyl sulfate-polyacrylamide gels (SDS-PAGE; Bio-Rad Laboratories SrL, Segrate, MI, IT). After electrophoresis

This item was downloaded from IRIS Università di Bologna (<https://cris.unibo.it/>)

When citing, please refer to the published version.

and transfer, nitrocellulose membranes (GE Healthcare Europe GmbH, Milano, MI, IT) were blocked for 1 h in 5% non-fat milk/0.1% Tween-20 in PBS (Sigma-Aldrich) at room temperature and incubated overnight at 4°C with primary antibodies (rabbit polyclonal anti-iNOS or anti-TREM2 1:1000 or mouse polyclonal anti-GAPDH, 1:20000, all from Santa Cruz Biotechnology) in 0.1% Tween-20/PBS. Membranes were then incubated with an anti-rabbit or anti-mouse secondary antibody conjugated to horseradish peroxidase (1:2000; Santa Cruz) for 90 min at RT in 0.1% Tween-20/PBS. Labeled proteins were detected by using the enhanced chemiluminescence method (ECL; BioRad) with a Chemidoc chemiluminescence detector (BioRad). Densitometric analysis was performed by using Image J software from NIH.

4.2.10. Statistical analysis. All results are the mean \pm S.E. of 3 different experiments. Statistical analysis was performed using the Graph Pad Prism 4 software by one-way ANOVA followed by Bonferroni post-hoc comparison test; p values less than 0.05 were considered statistically significant.

4.3. Molecular docking. Structure of compound **8** was constructed using build option within Discovery Studio 2.1. A single low energy 3D conformation was generated by energy minimization using the adopted based Newton-Raphson algorithm with the CHARMM force field [47].

The coordinates of hBuChE were obtained from the Protein Data Bank (PDB ID: 4BDS). Using protein model tool in Discovery Studio, version 2.1, software package, proper bonds, bond orders, hybridization and charges were assigned.

Cocrystal ligands and water molecules were removed and AutoDockTools (ADT; version 1.5.4) was used to add hydrogens and partial charges for proteins and ligands using Gasteiger charges.

This item was downloaded from IRIS Università di Bologna (<https://cris.unibo.it/>)

When citing, please refer to the published version.

All docking calculations were performed with the program AutoDock Vina [23] and they were applied to the whole protein target (*blind docking*). A grid box of 66 x 60 x 74 with grid points separated 1 Å was positioned in the middle of the protein (x = 136.0; y = 123.59; z = 38.56).

The first-ranked binding pose for the ligand in the active-site gorge cholinesterase was adopted in the present work for further analysis.

Acknowledgements

The experiments performed by AMM are part of his 665403 INCIPIT PhD programme, which is co-funded by the COFUND scheme Marie Skłodowska - Curie Actions.

References

- [1] M. Prince, A. Wimo, M. Guerchet, G-C. Ali, Y-T Wu, M. Prina, World Alzheimer disease report. Alzheimer's Disease International, London, UK, 25-46 (2015).
- [2] A. Contestabile, The history of the cholinergic hypothesis. Behav. Brain Res. 221 (2011) 334-340.
- [3] C. L. Masters, D. J. Selkoe, Biochemistry of amyloid β -protein and amyloid deposits in Alzheimer Disease, Cold Spring Harb. Perspect. Med. (2012) 2:a006262.
- [4] M. Jin, N. Shepardson, T. Yang, G. Chen, D. Walsh, D. J. Selkoe, Soluble amyloid β -protein dimers isolated from Alzheimer cortex directly induce Tau hyperphosphorylation and neuritic degeneration, Proc. Natl. Acad. Sci. U S A. 108 (2011) 5819–5824.

This item was downloaded from IRIS Università di Bologna (<https://cris.unibo.it/>)

When citing, please refer to the published version.

- [5] Y. Tang, W. Le, Differential Roles of M1 and M2 Microglia in Neurodegenerative Diseases, *Mol. Neurobiol.* 53 (2016) 1181-1194.
- [6] Z. Shen, X. Bao, R. Wang, Clinical PET Imaging of Microglial Activation: Implications for Microglial Therapeutics in Alzheimer's Disease, *Front. Aging Neurosci.* 10 (2018) 314.
- [7] J. R. Morphy, Chapter 10 The Challenges of Multi-Target Lead Optimization In: *Designing Multi-Target Drugs*; Morphy J.R. and C.J. Harris, Ed.; The Royal Society of Chemistry: London, 2012, pp. 141-154.
- [8] S. G. Fagan, V. A. Campbell, The influence of cannabinoids on generic traits of neurodegeneration, *Br. J. Pharmacol.* 171 (2014) 1347-1360.
- [9] V. Di Marzo, Endocannabinoids: synthesis and degradation, *Rev. Physiol. Biochem. Pharmacol.* 160 (2008) 1-24.
- [10] M. Mecha, F. J. Carrillo-Salinas, A. Feliú, L. Mestre, C. Guaza, Microglia activation states and cannabinoid system: Therapeutic implications, *Pharmacol. Ther.* 166 (2016) 40-55.
- [11] L. Tian, W. Li, L. Yang, N. Chang, X. Fan, X. Ji, J. Xie, L. Yang, L. Li, Cannabinoid Receptor 1 Participates in Liver Inflammation by Promoting M1 Macrophage Polarization via RhoA/NF- κ B p65 and ERK1/2 Pathways, Respectively, in Mouse Liver Fibrogenesis, *Front. Immunol.* 8 (2017) 1214.
- [12] B. G. Ramírez, C. Blázquez, T. Gómez del Pulgar, M. Guzmán, M.L. de Ceballos, Prevention of Alzheimer's disease pathology by cannabinoids: neuroprotection mediated by blockade of microglial activation, *J. Neurosci.* 25 (2005) 1904–1913.
- [13] Y. Tao, L. Li, B. Jiang, Z. Feng, L. Yang, J. Tang, Q. Chen, J. Zhang, Q. Tan, H. Feng, Z. Chen, G. Zhu, Cannabinoid receptor-2 stimulation suppresses neuroinflammation

- by regulating microglial M1/M2 polarization through the cAMP/PKA pathway in an experimental GMH rat model, *Brain Behav. Immun.* 58 (2016) 118-129.
- [14] X. Q. Luo, A. Li, X. Yang, X. Xiao, R. Hu, T. W. Wang, X. Y. Dou, D. J. Yang, Z. Dong, Paeoniflorin exerts neuroprotective effects by modulating the M1/M2 subset polarization of microglia/macrophages in the hippocampal CA1 region of vascular dementia rats via cannabinoid receptor 2, *Chin. Med.* 13 (2018) 14.
- [15] S. Rizzo, C. Rivière, L. Piazzzi, A. Bisi, S. Gobbi, M. Bartolini, V. Andrisano, F. Morroni, A. Tarozzi, J. P. Monti, A. Rampa, Benzofuran-based hybrid compounds for the inhibition of cholinesterase activity, β amyloid aggregation, and A β neurotoxicity, *J. Med. Chem.* 51 (2008) 2883-2886.
- [16] H. Khanam, S. Uzzaman, Bioactive Benzofuran derivatives: A review. *Eur. J. Med. Chem.* 97 (2015) 483-504.
- [17] D. R. Howlett, A. E. Perry, F. Godfrey, J. E. Swatton, K. H. Jennings, C. Spitzfaden, H. Wadsworth, S. J. Wood, R. E. Markwell, Inhibition of fibril formation in β -amyloid peptide by a novel series of benzofurans, *Biochem. J.* 340 (1999) 283-289.
- [18] C. C. Felder, K. E. Joyce, E. M. Briley, M. Glass, K. P. Mackie, K. J. Fahey, G. J. Cullinan, D. C. Hunden, D. W. Johnson, M. O. Chaney, G. A. Koppel, M. Brownstein, LY320135, a Novel Cannabinoid CB1 Receptor Antagonist, Unmasks Coupling of the CB1 Receptor to Stimulation of cAMP Accumulation, *J. Pharmacol. Exp. Therap.* 284 (1998) 291-297.
- [19] S. Rizzo, A. Tarozzi, M. Bartolini, G. Da Costa, A. Bisi, S. Gobbi, F. Belluti, A. Ligresti, M. Allarà, J.-P. Monti, V. Andrisano, V. Di Marzo, P. Hrelia, A. Rampa, 2-Arylbenzofuran-based molecules as multipotent Alzheimer's disease modifying agents, *Eur. J. Med. Chem.* 58 (2012) 519-532.

This item was downloaded from IRIS Università di Bologna (<https://cris.unibo.it/>)

When citing, please refer to the published version.

- [20] G. L. Ellman, K. D. Courtney, V. Andres, R. M. Featherstone, A new rapid colorimetric determination of acetylcholinesterase activity, *Biochem. Pharmacol.* 7 (1961) 88–95.
- [21] L.Y. Kong, M. K. McMillian, P. M. Hudson, L. Jin, J. S. Hong, Inhibition of lipopolysaccharide-induced nitric oxide and cytokine production by ultralow concentrations of dynorphins in mixed glia cultures, *J. Pharmacol. Exp. Ther.* 280 (1997) 61–66.
- [22] K. Pahan, A. M. Namboodiri, F.G. Sheikh, B.T. Smith, I. Singh, Increasing cAMP attenuates induction of inducible nitric-oxide synthase in rat primary astrocytes, *J. Biol. Chem.* 272 (1997) 7786–7791.
- [23] O. Trott, A. J. Olson, AutoDock Vina: improving the speed and accuracy of docking with a new scoring function, efficient optimization, and multithreading, *J. Comput. Chem.* 31 (2010) 455–461.
- [24] V. Andrisano, M. Naldi, A. De Simone, M. Bartolini, A patent review of butyrylcholinesterase inhibitors and reactivators 2010–2017, *Expert Opin. Ther. Pat.* 28 (2018) 455–465.
- [25] M. Mazzola, V. Micale, F. Drago, Amnesia induced by beta-amyloid fragments is counteracted by cannabinoid CB1 receptor blockade, *Eur. J. Pharmacol.* 477 (2003) 219–225.
- [26] N. M. de Bruin, J. Prickaerts, J. H. Lange, S. Akkerman, E. Andriambeloson, M. de Haan, J. Wijnen,; M. van Drimmelen,; E. Hissink, L. Heijink, C. G. Kruse, SLV330, a cannabinoid CB1 receptor antagonist, ameliorates deficits in the T-maze, object recognition and social recognition tasks in rodents, *Neurobiol. Learn. Mem.* 934 (2010) 522–531.
- [27] W.K. Hagmann, The many roles for fluorine in medicinal chemistry, *J. Med. Chem.* 51 (2008) 4359–4369.

This item was downloaded from IRIS Università di Bologna (<https://cris.unibo.it/>)

When citing, please refer to the published version.

- [28] F. Belluti, A. De Simone, A. Tarozzi, M. Bartolini, A. Djemil, A. Bisi, S. Gobbi, S. Montanari, A. Cavalli, V. Andrisano, G. Bottegoni, A. Rampa, Fluorinated benzophenone derivatives: balanced multipotent agents for Alzheimer's disease, *Eur. J. Med. Chem.* 78 (2014) 157-166.
- [29] F. Bonvicini, G. A. Gentilomi, F. Bressan, S. Gobbi, A. Rampa, A. Bisi, F. Belluti, Functionalization of the Chalcone Scaffold for the Discovery of Novel Lead Compounds Targeting Fungal Infections, *Molecules* 2019, 24(2). doi: 10.3390/molecules24020372.
- [30] E. Janefjord, J. L. Mååg, B. S. Harvey, S. D. Smid, Cannabinoid effects on β amyloid fibril and aggregate formation, neuronal and microglial-activated neurotoxicity in vitro, *Cell. Mol. Neurobiol.* 34 (2014) 31-42.
- [31] C. J. Pike, A. J. Walencewicz-Wasserman, J. Kosmoski, D. H. Cribbs, C. G. Glabe, C. W. Cotman, Structure-activity analyses of beta-amyloid peptides: contributions of the beta 25-35 region to aggregation and neurotoxicity, *J. Neurochem.* 64 (1995) 253–265.
- [32] A. S. Johansson, J. Bergquist, C. Volbracht, A. Päiviö, M. Leist, L. Lannfelt, A. Westlind-Danielsson, Attenuated amyloid- β aggregation and neurotoxicity owing to methionine oxidation, *Neuroreport* 18 (2007) 559–563.
- [33] E. Peña-Altamira, S. Petralla, F. Massenzio, M. Virgili, M. L. Bolognesi, B. Monti, Nutritional and Pharmacological Strategies to Regulate Microglial Polarization in Cognitive Aging and Alzheimer's Disease, *Front. Aging Neurosci.* 9 (2017) 175.
- [34] E. Peña-Altamira, F. Prati, F. Massenzio, M. Virgili, A. Contestabile, M. L. Bolognesi, B. Monti, Changing paradigm to target microglia in neurodegenerative diseases: from anti-inflammatory strategy to active immunomodulation. *Expert Opin. Ther. Targets.* 20 (2016) 627-640.

- [35] N. Stella, Endocannabinoid signaling in microglial cells, *Neuropharmacology* 56 (2009) (Suppl. 1), 244–253.
- [36] C. J. Fowler, M. L. Rojo, A. Rodriguez-Gaztelumendi, Modulation of the endocannabinoid system: neuroprotection or neurotoxicity?, *Exp. Neurol.* 224 (1) (2010) 37–47.
- [37] B. K. Atwood, K. Mackie, CB2: a cannabinoid receptor with an identity crisis, *Br. J. Pharmacol.* 160 (3) (2010) 467–479.
- [38] J. C. Ashton, M. Glass, The cannabinoid CB2 receptor as a target for inflammation-dependent neurodegeneration, *Curr. Neuropharmacol.* 5 (2007) 73–80.
- [39] D.R. Janero, A. Makriyannis, Cannabinoid receptor antagonists: pharmacological opportunities, clinical experience, and translational prognosis, *Expert Opin. Emerg. Drugs* (2009) 14 (1).
- [40] R. Ribeiro, J. Wen, S. Li, Y. Zhang, Involvement of ERK1/2, cPLA2 and NF-κB in microglia suppression by cannabinoid receptor agonists and antagonists, *Prostaglandins Other Lipid Mediat.* 100–101 (2013) 1–14.
- [41] W. Bu, H. Ren, Y. Deng, N. Del Mar, N. M. Guley, B. M. Moore, M. G. Honig, A. Reiner, Mild Traumatic Brain Injury Produces Neuron Loss That Can Be Rescued by Modulating Microglial Activation Using a CB2 Receptor Inverse Agonist, *Front. Neurosci.* 10 (2016) 449.
- [42] C. A. Lunn, E-P. Reich, J.S. Fine, B. Lavey, J. A. Kozlowski, R. W. Hipkin, D. J. Lundell, L. Bober, Biology and therapeutic potential of cannabinoid CB2 receptor inverse agonists, *Br. J. Pharmacol.* 153 (2008) 226–239.
- [43] N. A. Osman, A. Ligresti, C. D. Klein, M. Allarà, A. Rabbito, V. Di Marzo, K. A. Abouzid, A. H. Abadi, Discovery of novel Tetrahydrobenzo[b]thiophene and pyrrole based

This item was downloaded from IRIS Università di Bologna (<https://cris.unibo.it/>)

When citing, please refer to the published version.

- scaffolds as potent and selective CB₂ receptor ligands: The structural elements controlling binding affinity, selectivity and functionality, *Eur. J. Med. Chem.* 122 (2016) 619-634.
- [44] A. Rampa, M. Bartolini, L. Pruccoli, M. Naldi, I. Iriepa, I. Moraleda, F. Belluti, S. Gobbi, A. Tarozzi, A. Bisi, Exploiting the Chalcone Scaffold to Develop Multifunctional Agents for Alzheimer's Disease, *Molecules* 23 (2018) 1902.
- [45] A. Tarozzi, M. Bartolini, L. Piazzzi, L. Valgimigli, R. Amorati, C. Bolondi, A. Djemil, F. Mancini, V. Andrisano, A. Rampa, From the dual function lead AP2238 to AP2469, a multi-target-directed ligand for the treatment of Alzheimer's disease, *Pharmacol. Res. Perspect.* 2 (2014) e00023, doi:10.1002/prp2.23.
- [46] A. Rampa, S. Montanari, L. Pruccoli, M. Bartolini, F. Falchi, A. Feoli, A. Cavalli, F. Belluti, S. Gobbi, A. Tarozzi, A. Bisi, Chalcone-based carbamates for Alzheimer's disease treatment, *Future Med. Chem.* 9 (2017) 749–764.
- [47] B. R. Brooks, R. E. Bruccoleri, B. R. Olafson, D. J. States, S. Swaminathan, M. Karplus, CHARMM: A program for macromolecular energy, minimization, and dynamics calculations, *J. Comput. Chem.* 4 (1983) 187–217.